Biomedical Research Institute (BRI) - Foundation for Research and Technology-Hellas (FORTH), Ioannina, Greece

and

Laboratory of Biological Chemistry, Department of Medicine, University of Ioannina, Greece

Master's Thesis

Inter-institutional Interdepartmental Program of Postgraduate Studies
"Molecular and Cellular Biology and Biotechnology"

Study of the trafficking of Galectin-1, an unconventionally secreted protein.

Panagiotis Lentzaris, Biologist

Supervisor: Savvas Christoforidis, Professor of Biological Chemistry,

Department of Medicine, University of Ioannina

Ioannina 2024

Dedicated to the loving memory of my grandmother, Paraskevi...

Acknowledgements

CONTENTS

ABBREVIATION LIST

aa - Amino acids

ABC - ATP-binding cassette

Ang-2 - Angiopoietin-2

AU - Airy Units

CRD - Conserved recognition domain

ddH$_2$O - Double distilled water

EC - Endothelial cells

ECGS - Endothelial Cell Growth Supplement

ECM - Extracellular matrix

ER - Endoplasmic reticulum

FBS - Fetal Bovine Serum

Gal-1- Galectin-1

GBP - GFP binding protein

HMW - High molecular weight

HUVECs - Human umbilical vein endothelial cells

ICAM-1 - Intercellular adhesion molecule-1

IL - Interleukin

kDa - Kilodalton

LB - Luria Broth

LEL - Late endosome/lysosome

LMW - Low molecular weight

LPS - Lipopolysaccharide

LRO - Lysosome-related organelles

M199 - Medium 199

NTD - N-terminal domain

PBS - Phosphate Buffer Saline

PFA - Paraformaldehyde

PM - Plasma membrane

rpm - Revolutions per minute

RT – Room temperature

SD - standard deviation

SP - Signal peptide

STXBPs - Syntaxin-binding proteins

TGN - trans Golgi Network

UPS - Unconventional protein secretion

VEGFR - Vascular endothelial growth factor receptor

VWF - von Willebrand factor

WPBs - Weibel Palade bodies

ΠΕΡΙΛΗΨΗ

Η δυσλειτουργία του αγγειακού ενδοθηλίου εμπλέκεται στις πιο απειλητικές για τη ζωή ασθένειες, όπως είναι τα καρδιαγγειακά και φλεγμονώδη νοσήματα, καθώς και η καρκινική αγγειογένεση. Βιοδραστικά μόρια που σχετίζονται με τις παραπάνω ασθένειες και εκκρίνονται από τα ενδοθηλιακά κύτταρα, αρχικά αποθηκεύονται σε κυτταροειδικά εκκριτικά κυστίδια, τα επονομαζόμενα «Weibel-Palade bodies» (WPBs). Μέχρι σήμερα, έχει ταυτοποιηθεί μόνο ένα μέρος των πρωτεϊνών που απελευθερώνονται από τα WPBs. Για αυτό σε προηγούμενη έρευνα στο εργαστήριό μας, πραγματοποιήθηκε πρωτεομική ανάλυση στο υλικό που εκκρίνεται από ενεργοποιημένα ενδοθηλιακά κύτταρα (HUVEC). Προς έκπληξή μας, μεταξύ των νέων πρωτεϊνών που ταυτοποιήθηκαν, βρέθηκε και η πρωτεΐνη galectin-1 (Gal-1), η οποία είναι μια μη συμβατικά εκκρινόμενη πρωτεΐνη, με τον ακριβή μηχανισμό εξωκυττάρωσής της να μην είναι ακόμα γνωστός. Επιπλέον, αδημοσίευτα δεδομένα του εργαστηρίου έδειξαν ότι η Gal-1 εντοπίζεται σε ένα υποσύνολο των WPBs και σε περιορισμένο αριθμό κυττάρων HUVE.

Ο εντοπισμός της Gal-1 στα WPBs γεννά πολλά ενδιαφέροντα ερωτήματα. Αρχικά, στην παρούσα μελέτη θελήσαμε να διερευνήσουμε την ακριβή τοπολογία της Gal-1 στα WPBs. Ειδικότερα, δεδομένου ότι η Gal-1 είναι μια κυτταροπλασματική πρωτεΐνη, θεωρήσαμε σημαντικό να διερευνήσουμε αν η Gal-1 απλά αγκυροβολείται στην μεμβράνη των WPBs προς την κυτταροπλασματική τους πλευρά ή αν εισέρχεται στον αυλό των κυστιδίων. Η απάντηση του συγκεκριμένου ερωτήματος θα δώσει σημαντικές πληροφορίες για τη λειτουργία της Gal-1 στα συγκεκριμένα κυστίδια και την επακόλουθη πορεία της, μετά την επαγόμενη από προσδέτη εξωκυττάρωση των κυστιδίων.

Για την ακριβή τοπολογία, εξαιτίας της πολύ μικρής διαμέτρου των WPBs (100-300 nm) η οποία είναι σημαντικά μικρότερη από το διακριτικό όριο της συνεστιακής μικροσκοπίας (500nm), και άρα δεν επιτρέπει τη διάκριση μεταξύ της μεμβράνης και του αυλού των WPBs, τροποποιήσαμε το pH των κυστιδίων, κάτι που αυξάνει την διάμετρό τους, αφού μεταβάλλει το σχήμα τους από επίμηκες σε σφαιρικό, επιτρέποντας τελικά τον διαχωρισμό της μεμβράνης από τον αυλό. Υπό αυτές τις συνθήκες, πραγματοποιήσαμε τριπλή χρώση ανοσοφθορισμού για τον ενδογενή VWF (το κύριο πρωτεϊνικό φορτίο αυλού των WPBs), την EGFP-Rab27a (ένας μεμβρανικός

δείκτης των κυστιδίων) και την ενδογενή Gal-1. Η ανάλυση αυτή οδήγησε στο πολύ ενδιαφέρον εύρημα, πως η Gal-1 αποθηκεύεται στον αυλό των WPBs.

Επιπλέον, επιβεβαιώσαμε δεδομένα του εργαστηρίου από προηγούμενη έρευνα, ότι δηλαδή η Gal-1 αποθηκεύεται σε ένα υποσύνολο των WPBs και σε περιορισμένο αριθμό κυττάρων HUVE. Επίσης παρατηρήσαμε πως συχνά η Gal-1 αποθηκεύεται σε WPBs περίεργου (μη επίμηκους) σχήματος, τα οποία πιθανόν έχουν προκύψει από ομοτυπική σύντηξη μεταξύ ανεξάρτητων κυστιδίων. Αυτές οι παρατηρήσεις μας οδήγησαν στο να μελετήσουμε τις συνθήκες που επάγουν την είσοδο της Gal-1 στα WPBs. Βρήκαμε πως συσσώρευση των κυστιδίων στην περιφέρεια του κυττάρου, όπως συμβαίνει κατά την καλλιέργεια των κυττάρων σε συνθήκες υψηλής πυκνότητας (over-confluent cell culture conditions) ή κατά την κυτταρική μετανάστευση (cell migration), αυξάνει σημαντικά τον αριθμό των κυστιδίων που αποθηκεύουν την πρωτεΐνη Gal-1. Η αύξηση αυτή θα μπορούσε να οφείλεται σε ατελή ομοτυπική σύντηξη μεταξύ των κυστιδίων, κάτι που επάγεται από την υψηλή πυκνότητά τους. Τα δεδομένα αυτά καταδεικνύουν πως η Gal-1 εισέρχεται στα κυστίδια πιθανώς λόγω καταστροφής της μεμβράνης των κυστιδίων, ένας μηχανισμός εξωκυττάρωσης που έχει προταθεί βιβλιογραφικά για άλλους τύπους κυστιδίων από μη συμβατικά εκκρινόμενες πρωτεΐνες. Η σύνδεση της Gal-1 σε γλυκοζυλιωμένες πρωτεΐνες που βρίσκονται στον αυλό των WPBs θα μπορούσε να είναι μηχανισμός ρύθμισης της δράσης των εκκρινόμενων μορίων, ελέγχοντας με τον τρόπο αυτόν την προθρομβωτική, προφλεγμονώδη και αγγειογενετική δραστικότητα των εκκρινόμενων από τα κυστίδια, πρωτεϊνών.

ABSTRACT

Vascular endothelial dysfunction is implicated in the most life-threatening diseases, such as cardiovascular and inflammatory diseases, as well as cancer angiogenesis. Critical molecules in these diseases are derived from endothelial cells and are stored in Weibel Palade bodies (WPBs), which are endothelial specialized secretory organelles. To date, only a part of the WPBs-released proteins has been identified. Thus, previous work from our laboratory performed proteomic analysis on activated endothelial cells (HUVEC). Strikingly, among the new proteins identified was the protein galectin-1 (Gal-1), which is an unconventionally secreted protein, whose exact mechanism of exocytosis is not yet known. Unpublished work from our group showed that Gal-1 is localized in a sub-population of cells, in a sub-group of WPBs.

The localization of Gal-1 in WPBs sparks interesting questions. Firstly, we asked what is the precise topology of Gal-1 within the secretory WPBs. Given that Gal-1 is a cytoplasmic protein, it is critical to assess whether Gal-1 is simply docked at the cytoplasmic surface of WPBs, or it enters the lumen of these organelles. Addressing this question, would yield significant insights into the possible function of Gal-1 within these vesicles and its subsequent fate upon ligand-induced exocytosis.

To address the exact topology, due to the exceptionally diminutive diameter of the WPBs (100-300 nm) which is lower than the optical resolution of confocal microscopy (500 nm), we altered the pH of the vesicles, which increases their diameter by inducing their rounding and thereby allowing us to resolve between the lumen and the membrane of the vesicle. Under these conditions, we performed triple immunofluorescence staining for endogenous VWF (the main lumenal cargo protein), EGFP-Rab27a (a membrane marker of these vesicles) and endogenous Gal-1. Intriguingly, we found that Gal-1 is stored within the lumen of WPBs.

Furthermore, we confirmed previous lab findings that Gal-1 is stored in a sub-population of WPBs, in subset of cells. In often cases, Gal-1 positive bodies exhibited irregular shape, suggesting that they may arise from homotypic fusion between independent bodies. These observations prompted us to explore the conditions that trigger Gal-1 entry into these cellular compartments. We found that accumulation of vesicles in the periphery of the cell, as occurs during over-confluent cell culture conditions or during cell migration, leads to a significant increase in Gal-1 positive

WPBs. The increase in Gal-1 positive WPBs could be due to leaky homotypic fusion of vesicles, which is induced by their high density. This suggests that Gal-1 entry into vesicles is possibly due to damage to their membrane, a mechanism of exocytosis that has been suggested in the literature for other types of vesicles by unconventionally secreted proteins. Binding of Gal-1 to glycosylated cargo proteins in the lumen of WPBs could be a mechanism regulating the activity of secreted molecules, thereby controlling the prothrombotic, proinflammatory and angiogenic activity of secreted cargo.

1. INTRODUCTION

1.1 The Vascular Endothelium

The vascular endothelium, a single layer of endothelial cells (EC), constitutes the inner cellular lining of the blood vessels (arteries, veins and capillaries), placed at the interface of the blood circulation and vessel wall (Figure 1.1, A). Therefore, is in direct contact with the components and cells of blood. The endothelium shows polarity and is divided into two sides: the apical, which faces the lumen of the vessel, and the basolateral, which is in contact with the extracellular matrix (ECM) and adjacent tissues (Van Der Wouden et al., 2003). A layer called the endothelial glycocalyx, which is made up of a mosaic of glycoproteins, proteoglycans, and glycosaminoglycan chains, covers the apical surface of the endothelium (Luft, 1966). The endothelium surface layer is composed of the endothelial glycocalyx, secreted proteoglycans, and other adsorbed plasma proteins, such as albumin (Pries et al., 2000) (Figure 1.1,B).

In the 1950s the endothelium was considered to be merely a "cellophane wrapper" of the vessel wall, with the sole function of holding the contents of the vessel inside (Florey, 1966) . However, it is now well known that the endothelium is an active endocrine organ, which produces and releases compounds involved in a multitude of essential functions, which include regulation of vascular tone, blood coagulation and thrombosis, cellular adhesion, angiogenesis, and inflammation (Félétou & Vanhoutte, 2006; Goligorsky, 2005). Thus, there is a need for regulation to ensure smooth blood flow under normal conditions and an immediate response in case of blood vessel injury and infectious or inflammatory insults. To cope with this, endothelial cells are equipped with specialized secretory vesicles, called Weibel-Palade bodies (WPBs), which are ready-to-be-used, and store and secrete, after an appropriate stimulus, compounds necessary for responding to different conditions.
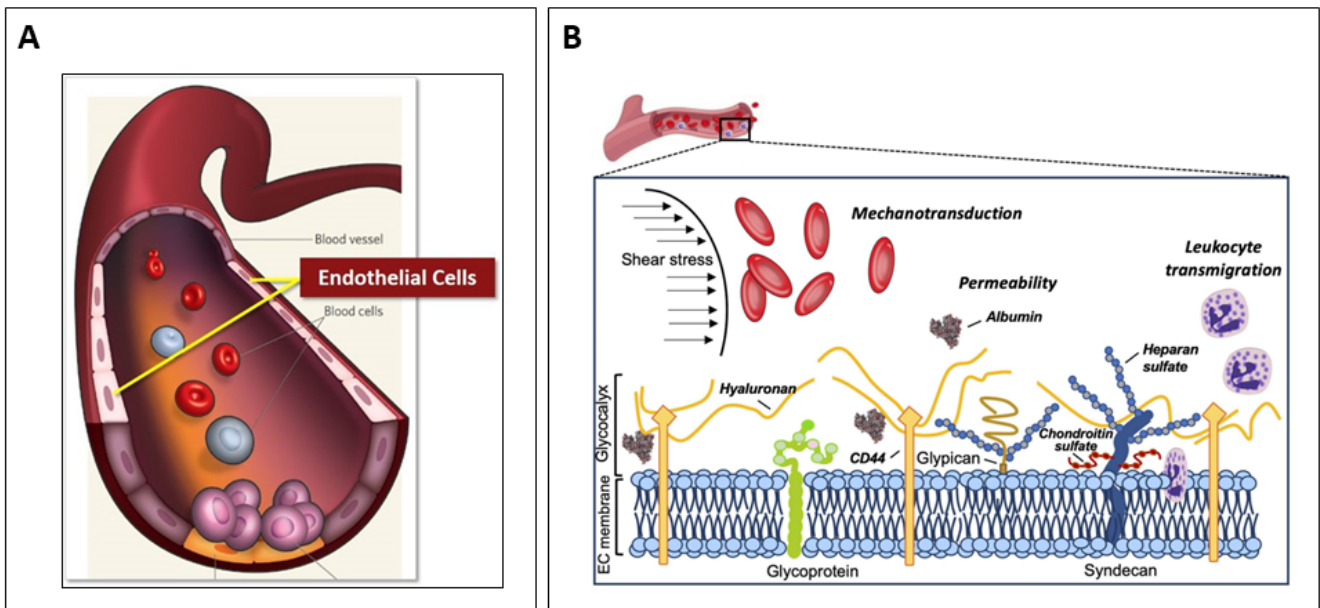
Figure 1.1- The vascular endothelium and the endothelial glycocalyx. *(A) Cross-sectional view of a blood vessel, showing the endothelial cells that form the inner layer of the vessel (Endothelial | Cell Applications. (n.d.). CELL APPLCATIONS, INC. Retrieved February 6, 2022, from https://www.cellapplications.com/endothelial). (B) The endothelial glycocalyx is represented schematically in terms of its essential elements (Villalba et al., 2021).*

1.2 Human umbilical vein endothelial cells (HUVECs)

Human umbilical vein endothelial cells (HUVECs) are a popular source of primary endothelial cells for *in-vitro* research, which, as their name suggests, are isolated from the umbilical cord's endothelium. The process of isolation is relatively easy, there are many available protocols (Baudin et al., 2007; Marin et al., 2001) for the isolation and maintenance with a relatively minimal requirement or they can be purchased from commercial resources. Furthermore, the source of the cells, i.e., the umbilical cord, is readily available as discarded biological waste after the child's birth. In addition to availability and ease of handling, HUVECs express many important endothelial markers (Caniuguir et al., 2016), e.g. ICAM-1, VEGFR and VWF, as well as signaling molecules associated with regulation of vascular homeostasis, such as NO (Boerma et al., 2006). Also, they respond to various physiological and pathophysiological stimuli, such as high glucose (Patel et al., 2013), lipopolysaccharide (LPS) administration (Jang et al., 2017) and shear stress (Walshe et al., 2013). All the above characteristics make them a general model for studying the endothelium, both in normal and diseased conditions. Last but not least, under proper conditions HUVECs

could also be successfully differentiated into 3D spheroid cultures (Heiss et al., 2015) and co-cultured in 3D systems with other cell types (Andrejecsk et al., 2013; Chowdhury et al., 2010) enabling the establishment of advanced models to better understand the behavior of ECs *in-vivo*. However, despite their many positive aspects and their extensive use in research, their importance for endothelial physiology is sometimes questioned, since they are derived from the umbilical cord, a tissue not found in non-neonatal individuals.

1.3 Weibel-Palade Bodies (WPBs)

As the endothelium is an active endocrine organ that must respond immediately (within seconds) to changes in the environment, for example in the case of vascular damage, the biomolecules secreted in response must be pre-stored in secretory vesicles ready for use. The endothelial secretory granule was first observed on Valentine's Day in 1962 by Ewald Weibel, when he was working in George Palade's laboratory (Weibel, 2012; Weibel & Palade, 1964). The researchers observed using electron microscopy "A hitherto unknown rod-shaped cytoplasmic component" (Weibel, 2012) and in their honor the vesicles were eventually named Weibel-Palade bodies (WPBs). These organelles are now a characteristic feature of endothelial cells. Also, they have been found in a range of vertebrates, including hagfish (Yano et al., 2007), according to subsequent research, which implies that they existed at least 500 million years ago.

WPBs are characterized in the literature as long, rod or cigar-shaped, cylindrical structures (Figure 1.2, A and B) with a diameter of 0.1–0.3 μm and a length of 1–5 μm (Michaux & Cutler, 2004; Weibel & Palade, 1964). Their main protein component is the pro-hemostatic protein von Willebrand factor (VWF) which is the first functional cargo of WPBs to be identified (Wagner, 1982). VWF is essential for the existence of WPBs. More specifically, VWF-deficient animals lack WPBs in their endothelial cells (Denis et al., 2001) whereas other cell types that express recombinant VWF are stimulated to form granules that resemble WPBs and have a similar cigar-shaped and striated appearance (Voorberg et al., 1993; Wagner et al., 1991). These data demonstrate that VWF can induce the elongated shape of vesicles due to its polymerization, a process that is discussed below. The second WPB cargo identified was P-selectin (Bonfanti et al., 1989), a membrane protein that initiates leukocyte recruitment in response to vascular injury when it appears in the apical plasma membrane of

endothelial cells. Therefore, WPBs control, at a minimum, the release of an important hemostatic factor as well as the appearance of a protein essential for the inflammatory response.

To date, a significant number of inflammatory and angiogenic mediators have been identified that are packaged in WPBs, with some being stored in the vesicle lumen (e.g. IL-8, Angiopoietin-2) and others located at the membrane (e.g. CD63, P-selectin). Some examples of cargo proteins and their topology (membrane or lumen) in the WPB, are shown in cartoon form in Figure 1.2, C. As vesicles store proteins with different roles, e.g. Angiopoietin-2 induces angiogenesis while interleukin (IL)-8 induces an inflammatory response, the simultaneous release of all proteins would be costly and even catastrophic for the organism. To adjust its secretory response to the current state of vascularity, the endothelium dynamically controls the content of WPBs by selectively incorporating or deleting specific cargos in response to signals from the surrounding microenvironment. For example, WPBs with conditions resembling laminar flow have lower levels of angiopoietin-2 (Ang-2) (Van Agtmaal et al., 2012). Furthermore, proinflammatory cytokine exposure causes chemokines like interleukin (IL)-8 and IL-6 to be upregulated, which are packaged into newly synthesized WPBs (Knipe et al., 2010). Due to WPBs' extended lifespan of around 24 hours (Giblin et al., 2008; Kobayashi et al., 2000), endothelial cells will gather different granule populations with varying quantities of cotargeted WPB cargo. Intriguingly, it has been proposed that certain subsets of granules may undergo differential exocytosis (Cleator et al., 2006); nevertheless, the exact mechanism underlying this differential release is yet unknown.
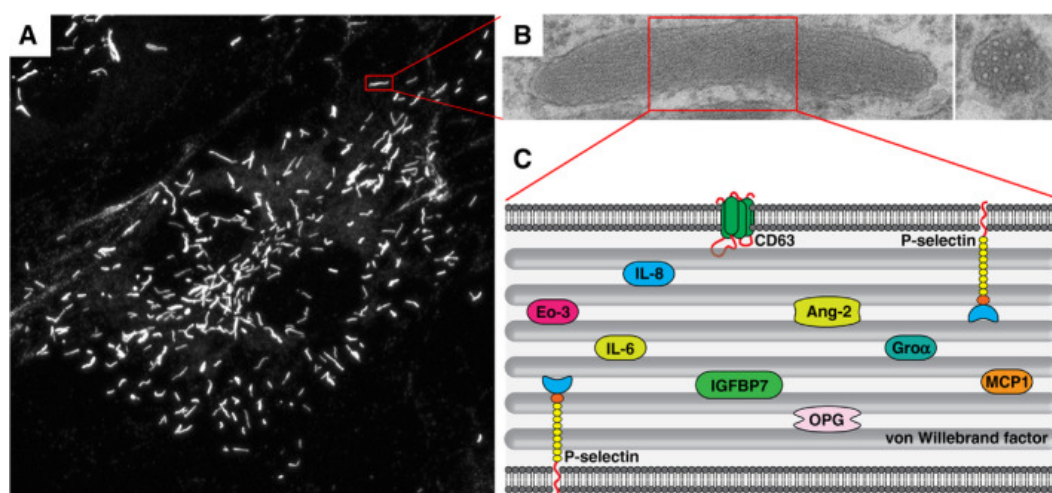
Figure 1.2 - Morphology of WPBs in nonstimulated endothelial cells *(A) Immunofluorescence image, using a-VWF antibody, showing the many elongated WPBs that are present in the cell. (B) WPB ultrastructure, left part: a longitudinal section showing internal striations, right part: a cross-section showing bundles, which represent densely packed VWF tubules. (C) Illustration of WPB cargo in a cartoon. Ang-2, angiopoietin-2; Eo-3, eotaxin-3; GROa, growth regulated oncogene a; IGFBP7, insulin-like growth factor-binding protein 7; IL-6, interleukin-6; IL-8, interleukin-8; MCP-1, monocyte chemoattractant protein-1; OPG, osteoprotegerin (Schillemans et al., 2019).*

A special feature of WPBs is that two or more vesicles can be fused, leading to the formation of irregularly shaped WPBs. Some examples of WPBs with strange shapes created after homotypic fusion are shown in the Figure 1.3. Fusion can occur at the edges or along the axes of the vesicles (Figure 1.3) (Valentijn et al., 2008).
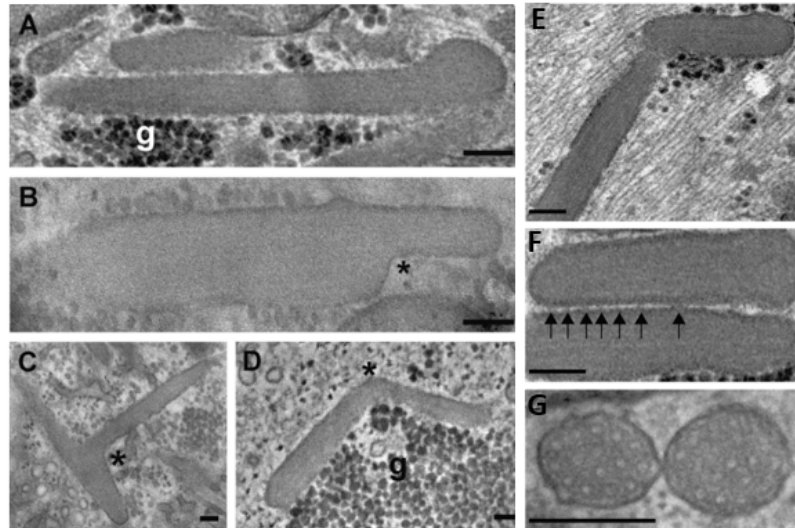
Figure 1.3 - Homotypic fusion of WPBs. *(A-D) 2D electron microscopy images showing WPBs with irregular shapes created after homotypic fusion. Asterisks indicate curvature with sharp angles of delimiting membranes and the letter g denotes glycogen islands. (E-G) 2D electron microscopy images of two WPBs, showing the fusion points between them. Fusion occurs (E) at the edges, (F) along their axes (arrows depict points of intense electron density representing contact points), and (G) cross-sectional view of two WPBs in close contact. (A-G) Scale bars = 100 nm. Modified image from (Valentijn et al., 2008).*

1.3.1 Biosynthesis of VWF and WPB formation

VWF is a large glycoprotein that is synthesized at the endoplasmic reticulum (ER) as pre-pro-VWF. In this cellular compartment, the signal peptide of 22 amino acids (aa) located at the amino-terminal end of the protein, responsible for targeting the protein to the endoplasmic reticulum, is cleaved to give a precursor, pro-VWF. The pro-VWF molecule is composed of conserved structural domains in the order D1-D2-D'-D3-A1-A2-A3-D4-B1-B2-B3-C1-C2-CK (Pannekoek & Voorberg, 1989) or, according to more recent studies, in the sequence D1-D2-D'-D3-A1-A2-A3-D4-C1-C2-C3-C4-C4-C5-C6-CK (Zhou et al., 2012). Domains D1D2 of 741 aa represent the propeptide, and the remaining domains, which span from domain D' to the cysteine knot (CK) domain, indicate mature VWF (Figure 1.4). Each VWF molecule contains an unusually high content of cysteine amino acids (8.2%), almost four times the average observed in

other human proteins (2.3%) (Shapiro et al., 2014). Cysteine residues form disulfide bonds between VWF molecules, which allows for its strong condensation inside WPBs.
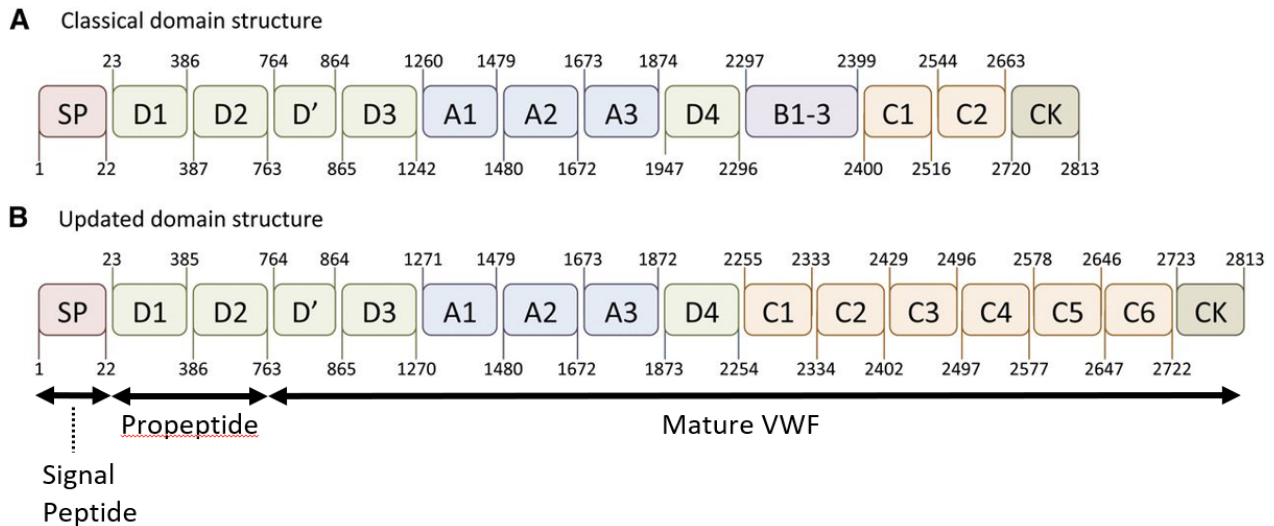
***Figure 1.4- Schematic view of pre-pro-VWF according to the old and new domain arrangement.** (A) The arrangement of repeating patterns according to the classical (old) model. (B) The new arrangement, according to which the addition of six homologous C domains to the B1-3-C1-C2 domain area is a notable alteration from the original domain structure. The numbers correspond to the residue numbers of the protein. At the bottom of the figure, the three arrows present the main parts of the pre-pro-VWF molecule: the Signal peptide, the propeptide (domains D1D2) and the mature VWF molecule (domains D'-CK). Modified image from (Lenting et al., 2015).*

In the ER, pro-VWF molecules form dimers by creating disulfide connections between CK domains at the C-terminus (Katsumi et al., 2000), i.e. "tail-to-tail" dimerization (Figure 1.5, part 2). The dimers then move from the ER to the Golgi apparatus. Due to the acidic pH and Ca^{2+} ions in the Golgi (Paroutis et al., 2004), dimers reorganize into what are known as "dimeric bouquets", in which the dimers are aligned into a side-by-side manner (Zhou et al., 2011). In this domain, the amino-terminal D1-D3 domains create a more globular shape to produce the "flower," and their middle to carboxyl domains closely couple into a rod-like "stalk" (Figure 1.5, part 3). Due to the trans-Golgi lumenal conditions, the dimers can also be stacked into a right-handed coil (Huang et al., 2008) (Figure 1.5, part 4). Here, the interaction between the D1-D3 domains from juxtaposed dimers forms the heart of a tubule, and the stalks protrude like a bottlebrush. As a result of the dimers' proper alignment, further disulfide

bonds can be formed between the D3 regions located at the N-terminus ("head-to-head" multimerization), leading to the creation of multimers, a process that is catalyzed by the propeptide (Figure 1.5, parts 5,6). The involvement of the propeptide is essential, as multimerization is impossible in its absence (Verweij et al., 1987). In the trans Golgi Network (TGN), although there is cleavage of the propeptide by furin (Wise et al., 1990), propeptide and mature VWF are still being linked by non-covalent bonds, in a 1 :1 stoichiometric ratio (Ewenstein et al., 1987). In addition to the cleavage of propeptide, additional post-translational modifications, such as N- and O-glycosylation, occur in the TGN (Canis et al., 2012; Samor et al., 1989). Finally, it is important to note that VWF tubulation allows VWF to be compressed inside the WPBs, approximately 45 times (McCormack et al., 2017).
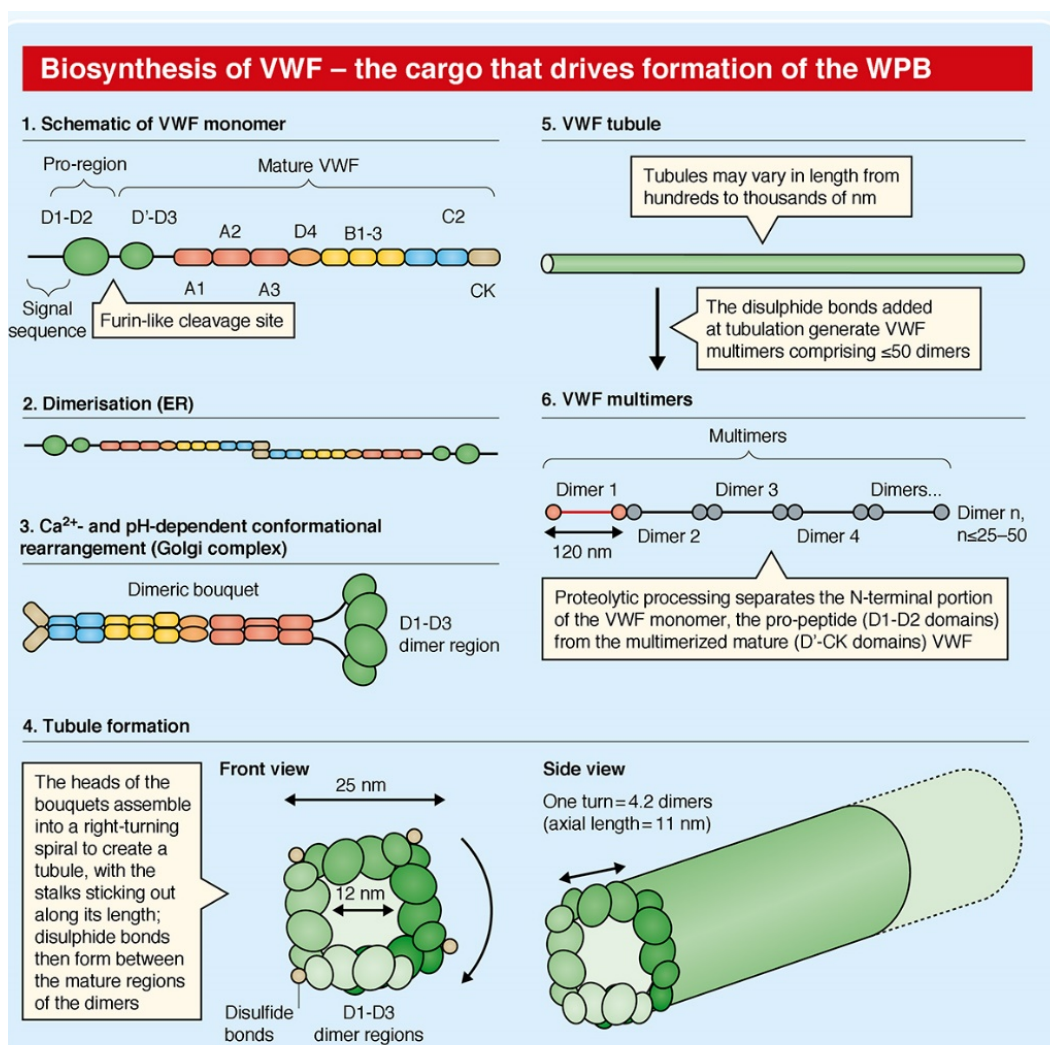
Figure 1.5 - Cartoon representation of the structures that VWF receives during the process of its organization into tubules. *The image also shows the cellular topology where each structure is obtained. Detailed description of the structures and the intra-molecule bonds that lead to the stabilization of the molecule, in the main text (McCormack et al., 2017).*

1.3.2 WPBs maturation

VWF polymerized in the TGN, either before or concurrently with the actual budding of immature WPB, maintains connections to the Golgi for 2-4 h, period that allows for more VWF polymerization and storage of other cargo proteins in the immature WPB (Mourik et al., 2015). WPBs released from the TGN further mature to eventually give rise to the highly elongated cigar-shaped organelles which are detected mainly in the periphery of endothelial cells.

The maturation of the WPB involves further polymerization of VWF inside the WPB in the form of tubules, which ultimately gives the unique rod-shaped organelle. Indeed, under the electron microscope, VWF in mature WPBs is distinguished in the form of internal striations/tubules, of intense electronic density and oriented parallel to their longitudinal axis in longitudinal section, while in transverse section the tubules appear as 'rings' with a vacant core surrounded by a space of intense electronic density (Valentijn et al., 2008) (Figure 1.6).
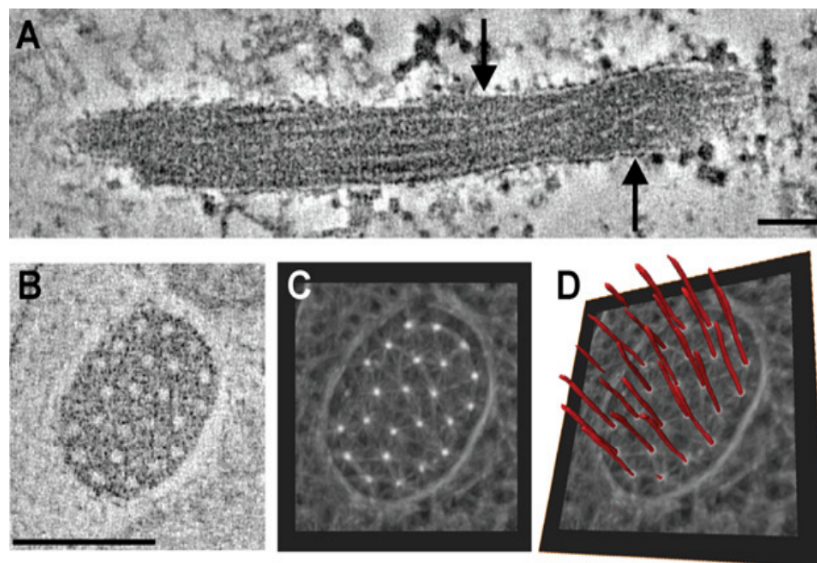
Figure 1.6- VWF is polymerized inside WPBs into tubular structures. (A). Electron tomography of a longitudinally arranged WPB and (B) transverse section of a WPB (Scale bars = 100 nm). (C, D) Modeling of VWF tubules in transverse section. Part of the image from (Valentijn et al., 2008).

During maturation there is also acquisition of additional cytosolic and endosomal/lysosomal components, such as RabGTPase Rab27a and tetraspanin CD63, designating WPB as lysosome-related organelles (LRO) (Bowman et al., 2019) (Figure 1.7, part 3). The biogenesis of lysosome related organelle-2 (BLOC-2) protein complex is essential for the transport of these proteins, as depletion of BLOC-2 results in both hampered CD63's transit from late endosome/lysosome (LEL) to WPB and widespread abnormalities in WPB maturation, where the WPB appears rounded rather than elongated and grouped in the perinuclear area (Ma et al., 2016; Sharda et al., 2020). In this phase, WPBs move in a microtubule-dependent manner to the cell periphery where they anchor to actin filaments (Figure 1.7, parts 2 and 3). The recruitment process of WPBs' exocytotic machinery required for the fusion and eventual exocytosis of WPBs is described in detail in the next section (Figure 1.7, parts 3,4 and 5, Figure 1.8)

As a result, the process of WPB maturation is extremely intricate and involves *de novo* protein acquisition, the transfer of proteins from LEL to WPB, and morphological changes that ultimately result in the production of a distinct organelle with a rod-like form that houses the tubulated, highly multimeric VWF.
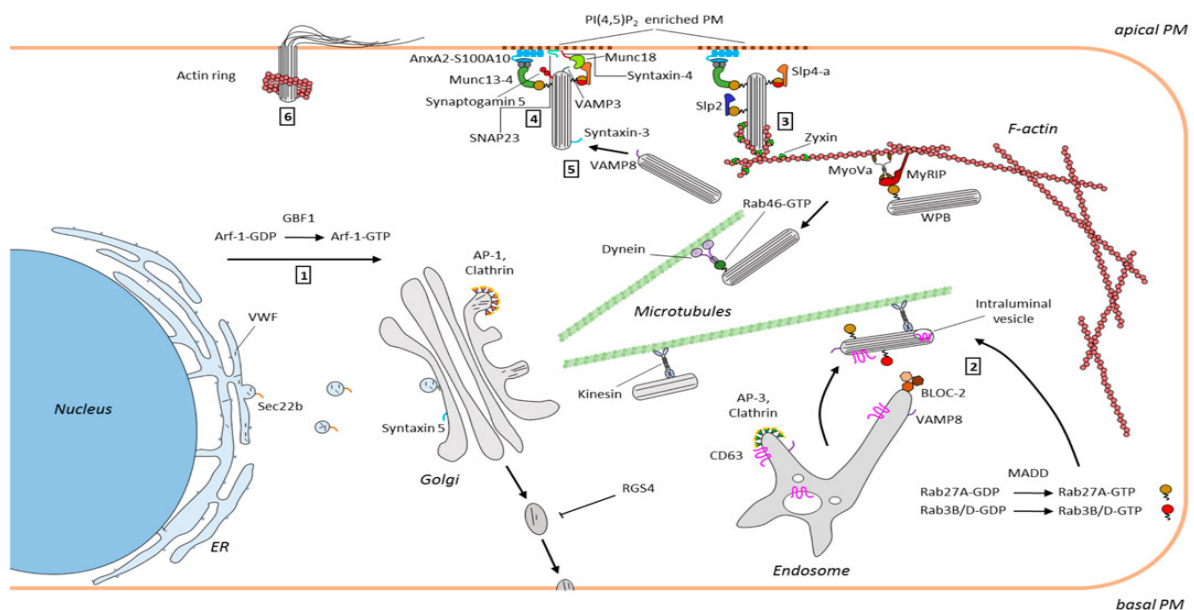
***Figure 1.7- Formation and maturation process of WPBs in endothelial cells.** The individual stages are distinguished: (1) VWF, which is produced at the ER and transported to the Golgi, drives WPB formation. (2) Following their bud from the TGN, WPBs are carried by microtubules to the cell periphery. Alongside this occurs the transfer of endosomal components including VAMP8 and CD63 to WPB, which is dependent on annexin A8 and BLOC-2. (3) Maturing WPBs acquire certain RabGTPases, such as Rab27A and Rab3, which are necessary for attaching WPB to the cortical actin cytoskeleton and facilitating exocytosis. (3,4 and 5) WPB tethering at and fusion with the PM requires many factors, including the annexin A2/S100A10/Munc13-4 complex and a SNARE-based fusion machinery. (6) Lastly, it has been shown that post-fusion actin rings facilitate the complete release of highly multimeric VWF. (Naß et al., 2021).*

1.3.3 WPBs' exocytotic machinery

During the maturation process described above, WPBs in addition to cargo proteins acquire parts of the exocytotic machinery (Bierings et al., 2012). More specifically, WPBs recruit several Rab family GTPases, such as Rab15, Rab27A, and various Rab3 isoforms (Zografou et al., 2012). A group of effector proteins (MyRIP, Munc13-4, and Slp4-a) are subsequently recruited to the WPB by the Rabs, when they are in their active GTP-bound state, by means of which WPBs interact with the cytoskeleton and/or the plasma membrane to eventually be secreted (Bierings et al., 2012; Nightingale et al., 2009; Zografou et al., 2012) (Figure 1.8). MyRIP is an effector unique to Rab27A that binds actin both directly and through the actin motor protein myosin Va and attaches WPBs to the actin cytoskeleton at the periphery of cells (Nightingale et al., 2009) (Figure 1.8). The release of WPBs involves conflicting functions of the actin cytoskeleton. One the one hand, it is required for the peripheral distribution of WPBs, which is dependent upon myosin IIa and is crucial for releasability (Li et al., 2018). However, actin also functions as a barrier (Vischer et al., 2000), and in this case MyRIP functions as a brake during exocytosis (Conte et al., 2015) by attaching WPBs to the actin cytoskeleton. Munc13-4 binds to both Rab27A and Rab15 (Zografou et al., 2012) and induces the tethering of WPB to the plasma membrane, after interaction with the annexin A2-S100A10 complex (Chehab et al., 2017) (Figure 1.8). Slp4-a interacts with Rab3 isoforms and Rab27A and promotes WPB exocytosis (Bierings et al., 2012), providing the link between WPB and the SNARE complex (Van Breevoort et al., 2014), which leads to the fusion of WPB to the plasma membrane (Figure 1.8). The formation of SNARE complexes is controlled by syntaxin-binding proteins (STXBPs).

1.3.4 Pathways of VWF secretion −polarity and multimeric state

The secretion of VWF takes place from both the apical and basolateral side of the endothelial cells. There are three main routes of VWF secretion: constitutive and basal secretion, both of which occur in the absence of stimulation, and regulated secretion that happens in response to an endothelial stimulus. Apart from the requirement on stimulus for exocytosis, the three pathways differ in the degree of polymerization of the VWF that is secreted and the polarity of release, i.e. whether it is secreted on the apical or basolateral side of the endothelium.
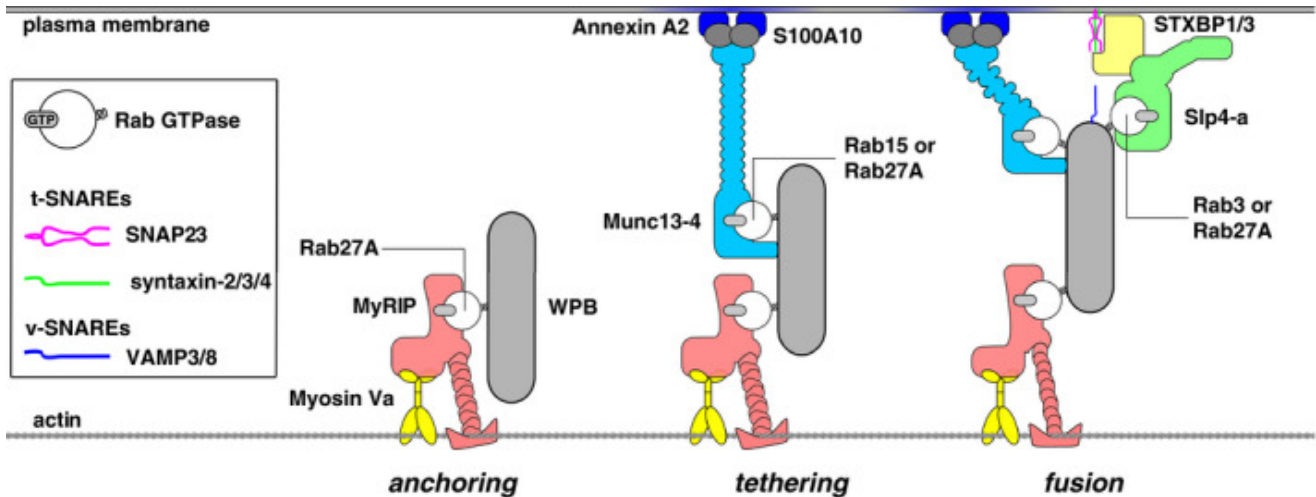
Figure 1.8 -Components of WPBs' exocytotic machinery on the pathway to fusion of WPB to the plasma membrane, which eventually leads to exocytosis. *The three key steps include (i) anchoring of WPB to the actin cytoskeleton via Rab27A-MyRIP-myosin Va complex, (ii) tethering to the plasma membrane via Rab27A-Munc13-4- annexin A2-S100A10 complex and (iii) fusion between WPB and the plasma membrane via SNARE proteins, through the interaction of Rab27A-Slp4 complex with members of the syntaxin-binding protein (STXBP) family (Schillemans et al., 2019).*

Following the constitutive secretion, low molecular weight (LMW) VWF multimers in the TGN are secreted via small short-lived vesicles, not storage WPBs, which are immediately released into the PM, without the requirement of a stimulus (Sporn et al., 1986). This secretion occurs mainly on the basolateral side of the endothelium (Lopes Da Silva & Cutler, 2016) (Figure 1.9).

Basal secretion is the mechanism by which most unstimulated VWF, of high molecular weight (HMW) multimers, is released (Zenner et al., 2007). Since VWF retention in this pathway correlates with the stated half-life of these granules, this most likely represents a slow, stochastic turnover of WPBs. At baseline, WPBs' secretory machinery is already somewhat prepared to handle low-level, spontaneous release (Giblin et al., 2008). This pathway release VWF primarily at the apical face of the cell (Lopes Da Silva & Cutler, 2016) (Figure 1.9).

Regulated secretion, similar to basal secretion, results in the release of high molecular weight (HMW) multimers of VWF(Zenner et al., 2007) and occurs primary at the apical side of the endothelium (Lopes Da Silva & Cutler, 2016) (Figure 1.9). In this case, however, an endothelial stimulus is required. Endothelial stimulation can be elicited by a plethora of agonists, such as thrombin, histamine, epinephrine (Lowenstein et al., 2005), which usually cause an increase in intracellular Ca^{2+} or cAMP levels,

which act as second messengers, mobilize the WPB that is cortically attached, and start the process of tethering/docking at the plasma membrane (PM).
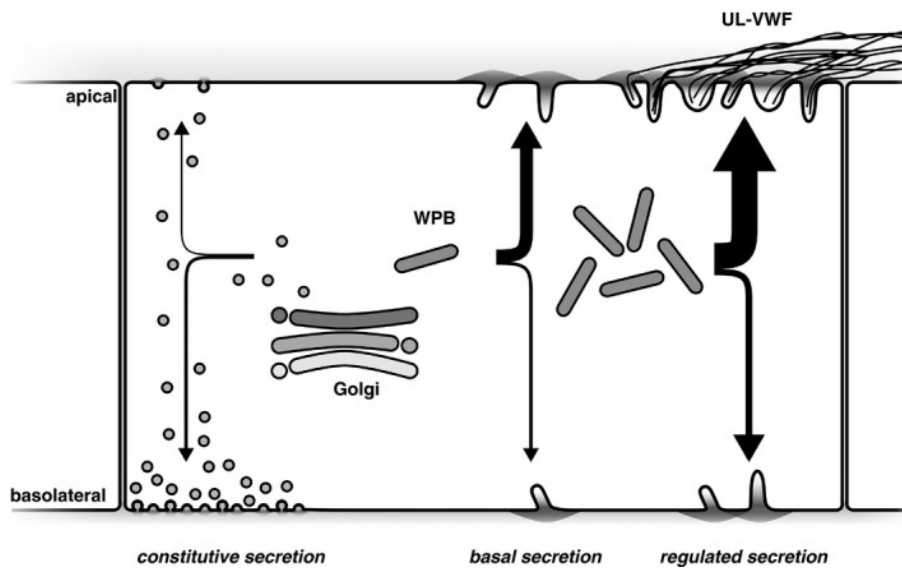
Figure 1.9- The three VWF secretion pathways of the endothelium and their polarity. *From left to right: (i) constitutive secretion of low molecular weight VWF, mostly expelled at the endothelium's basolateral side; and (ii) basal and (iii) regulated secretion of VWF with a high molecular weight from Weibel-Palade bodies (WPBs), mostly towards the apical surface. Ultralarge VWF (UL-VWF) multimers form from the several WPBs that undergo exocytosis during triggered release, and these multimers combine into VWF strings that function as adhesive platforms for platelets, on the apical side of the endothelium (Schillemans et al., 2019).*

1.3.5 Modes of exocytosis of WPBs

It is possible WPBs to employ several exocytosis modes, leading to the release of different types and amounts of cargo.

First, a full fusion of a single WPB with the plasma membrane ("Single WPB exocytosis"- Figure 1.10) can occur, leading to the collapse of the vesicle membrane and its related membrane components into the plasma membrane and the transport of soluble granule cargo, including VWF, into the lumen (Erent et al., 2007). For exocytosis it is possible to form an actin-myosin ring that helps the complete release of the WPB content (Nightingale et al., 2011) (the ring is shown schematically on Figure 1.7, part 6).

In the second mode of exocytosis, the so-called "lingering-kiss exocytosis" (Figure 1.10), although the WPB fuses with the plasma membrane, the pore remains in a restricted state for some seconds before closing prematurely. The restricted diameter

of the pore acts as a molecular size filter which only permits the secretion of cargo molecules less than ∼40 kDa and ions (e.g. H$^+$). So, small cargoes, such as chemokines can pass through the small pore, but larger cargo proteins such as VWF and VWF propeptide are not. There is also selectivity in membrane cargos, with CD63 being able to be transported to the plasma membrane while P-selectin is excluded from transport (Babich et al., 2008).

According to the third mode of exocytosis ("Multigranular exocytosis"- Figure 1.10), at a single fusion site, there can be several WPBs, which fuse homotypically and form enlarged, rounded structures, termed secretory pods, which contain disordered VWF tubules (Valentijn et al., 2010). VWF strings may finally arise from the extruded material, even though the tubular organization of VWF multimers in the spherical secretory pods has been lost (Mourik et al., 2013) (Figure 1.10). A related but mechanistically distinct mode of homotypic WPB fusion, termed "cumulative exocytosis" (not shown on the Figure 1.10) has been observed. In this mode, a post-fusion WPB serves as a site of membrane fusion for the cumulative fusion of other WPBs in succeeding steps (Kiskin et al., 2014).
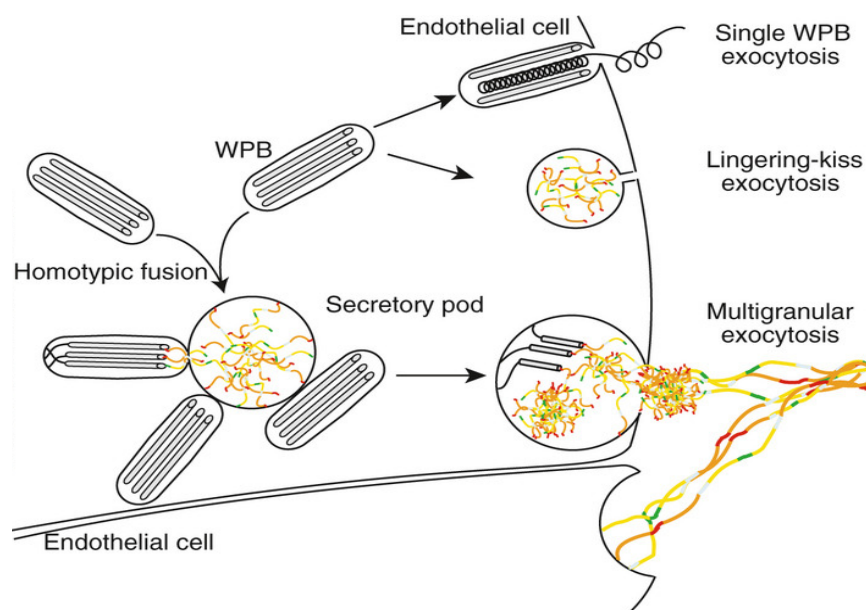
Figure 1.10- The different modes of WPB exocytosis. *(Top) "Single WPB exocytosis": a single WPB fuses with the plasma membrane and all cargoes, included VWF, are secreted. (Middle) "Lingering-kiss exocytosis": WPBs fuse with the plasma membrane, round up and a narrow pore is formed, allowing the secretion of only small cargoes. (Bottom) "Multigranular exocytosis": a secretory pod is formed, after WPBs homotypic fusion, which pools VWF molecules prior to secretion. Part of the figure from (Valentijn & Eikenboom, 2013).*

1.4 Brief review of conventional and unconventional secretion pathways

The conventional secretory pathway is used for the secretion of most proteins, and as such, it is a well-characterized pathway. In this case, the proteins have an **N-terminal signal sequence (signal peptide, SP) and/or a transmembrane domain that direct their insertion into the ER.** Then, proteins are transported by membrane-bound vesicles from the ER to the Golgi apparatus and ultimately to the cell surface (Nickel & Rabouille, 2009; Palade, 1975) (Figure 1.11).
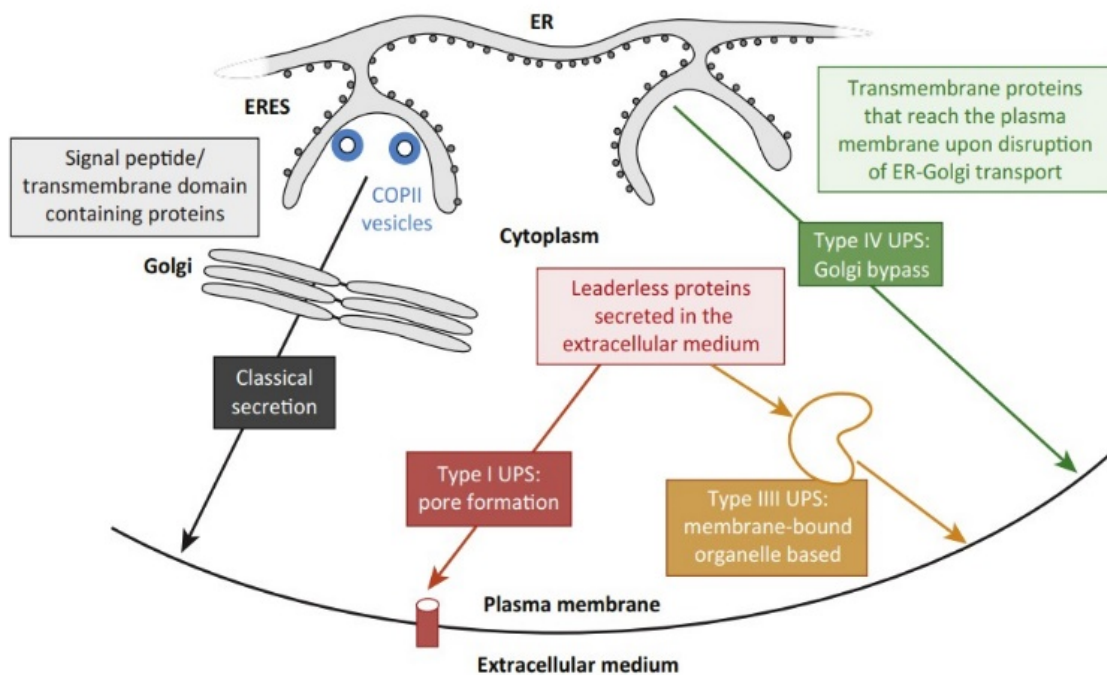
Figure 1.11- Schematic representation of conventional and unconventional secretion. *In black is shown the pathway of conventional (classical) secretion, in which proteins are moved by vesicles from the ER through the Golgi apparatus to the plasma membrane. The other three pathways correspond to the different types of unconventional protein secretion: (brown) Type I whereby proteins pass the plasma membrane through a pore, (orange) Type III whereby proteins use organelles (autophagosome or endosome) for secretion, (green) Type IV whereby secreted proteins enter the ER and reach the plasma membrane, bypassing the Golgi apparatus. Type II of unconventional secretion is not shown on the figure (Rabouille, 2017).*

However, several proteins (examples summarized on Table 1.1) that deviate from the conventional ER-Golgi-plasma membrane route have been found, which are secreted unconventionally, following a variety of distinct secretory pathways (Figure 1.11). There are four main categories of unconventional protein secretion (UPS) that are further divided into vesicular and non-vesicular pathways. The non-vesicular

pathways are classified to Type I, whereby proteins are transported across the plasma membrane through pores, assisted by other protein complexes or unfacilitated, and Type II, according to which ATP-binding cassette (ABC) transporter proteins facilitate translocation. The vesicular pathways are further divided into Type III and Type IV. Type III is an autophagosome-based or endosome-based secretion that these organelles are diverted from their normal function and become secretory, i.e. the secreted protein first enters the lumen of an organelle, which then fuses with the plasma membrane. According to Type IV secretion pathway, although secreted proteins do have signal peptide and/or a transmembrane domain and thus enter the ER, they bypass the Golgi apparatus to reach the plasma membrane (Rabouille et al., 2012).

Protein	Proposed secretion mechanism
FGF1	Non-vesicular
FGF2	Non-vesicular
Interleukin 1β	Vesicular
Galectins 1 and 3	Vesicular / Non-vesicular
HMGB1	Vesicular
AcbA	Vesicular
Thioredoxin	Non-vesicular
Engrailed Homeoproteins	Vesicular
HIV Tat	Non-vesicular
Tubby	Unclear
Yeast MATa	Non-vesicular

Table 1.1- Examples of unconventionally secreted proteins that have significant effects on health and disease. The proteins use vesicular or non-vesicular secretion mechanism, depending on their need for vesicular carrier for exocytosis. Part of the Table of (Manjithaya & Subramani, 2011).

1.5 Galectins

Galectins constitute a large family of galactose-specific lectins that bind β-galactosides via their conserved recognition domain (CRD) (Barondes et al., 1994). Based on their CRD domain structures, mammalian galectins are classified into three groups: prototypical, tandem repeat and the chimeric group consisting only of galectin-3 (Figure 1.12). Prototypical galectins have one CRD domain per polypeptide and form homodimers by non-covalently linking. Tandem repeat galectins are composed of two CRDs with different specificities to each other, which are connected by an unstructured linker peptide. The chimeric group consisting only of galectin-3, which has one CRD on the C-terminus and a large, flexible N-terminal domain (NTD).

An important feature of Galectins is that they lack a signal peptide and thus they are secreted unconventionally, with the exact mechanism of secretion not yet known (Popa et al., 2018). They have many functions outside of the cell, including binding plasma membrane proteins, interacting with extracellular matrix (ECM) components (Elola et al., 2007), inducing apoptosis (Stillman et al., 2006), evolving in epithelial homeostasis and as chemoattractants in the immune system (Henderson & Sethi, 2009; Vasta, 2012; Viguier et al., 2014). To perform their specialized roles, galectins require strict regulation of their secretion, which are based on the kind of cell in which they are expressed as well as their cellular or extracellular location.

In addition to their extracellular activities, galectins have also important functions inside the cells. In particular, they participate in intracellular trafficking, directing the stabilization and sorting of glycoproteins to their destination (Delacour et al., 2009). Furthermore, recent studies have shown that galectins accumulate around damaged endocytic vesicles, including damaged phagosomes, endosomes and lysosomes, inducing cellular responses such as autophagy and antimicrobial protein uptake (Hong et al., 2021)

Figure 1.12- Schematic representation of galectin family groups and formation of galectin-glycan structures*. Galectins can be divided into three groups: (a) prototypical, which have one CRD and form homodimers, (b) chimeric, which include only galectin-3, containing one CRD and a flexible N-terminal domain and forms pentamers upon binding to multivalent carbohydrates, (c) tandem repeat, which have two distinct CRDs connected by a linker. (Yang et al., 2008)*

Galectin-1 (Gal-1) is the first member of the galectin family to be identified. The protein is 135 amino acids in length (14-kDa) and since it belongs to the prototypical group, it forms homodimers, folding in a sandwich of two anti-parallel β-sheets, with two galactoside-binding sites (Figure 1.13). Gal-1 can be found within the nucleus, the cytoplasm, on the cell surface, and in the ECM, after secretion (Camby et al., 2006). Numerous cell processes are controlled by Gal-1, including immune responses, apoptosis, inflammation, intercellular and cell-matrix interaction, proliferation, migration, and adhesion, as well as carcinogenesis (Cousin & Cloninger, 2016; Fajka-Boja et al., 2016; Sundblad et al., 2017). Similar to all members of the galectin family, Gal-1 has no signal peptide to drive the protein into the conventional

ER-Golgi-plasma membrane pathway for exocytosis, so is unconventionally secreted. The exact mechanism of secretion has not yet been identified (Popa et al., 2018).
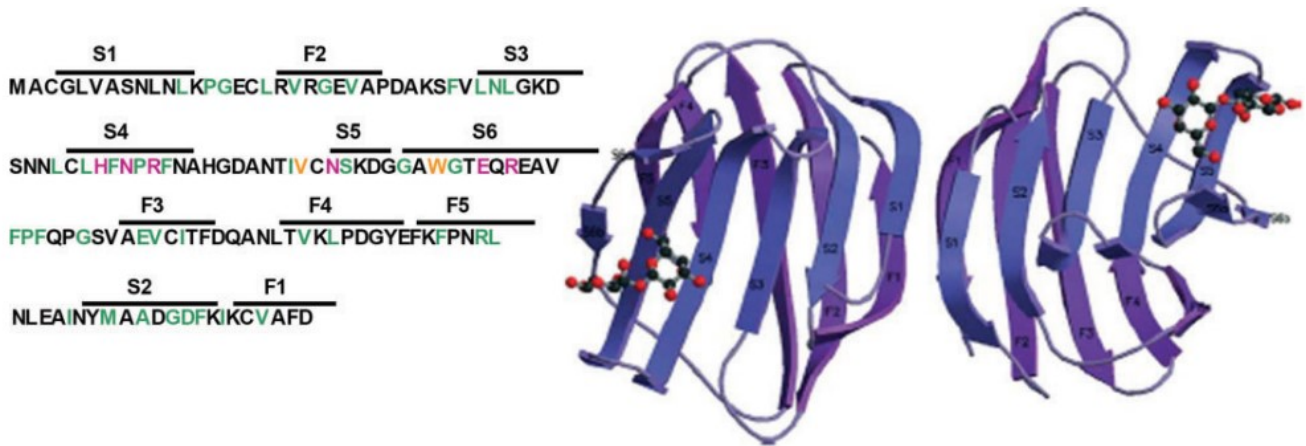
Figure 1.13- Structure of Gal-1 protein. (Left part) The amino acid sequence of the protein, consisting of 135 amino acids. The green amino acid symbols correspond to highly conserved residues, the pink ones correspond to the residues of the CRD structure that interact with carbohydrates via hydrogen bonds and the orange ones that interact with carbohydrates via van der Waals interactions. (right part) The overall folding of Gal-1 involves a β sandwich consisting of two anti-parallel β-sheets. Each monomer's N and C terms are positioned at the dimer interface, and the CRDs are situated at the far ends of the same face. This arrangement creates a long, negatively charged cleft in the cavity. (Camby et al., 2006)

1.6 Previous work in our lab identified galectin-1 in WPBs

The vascular endothelium, as described in detail in section 1.1, is an active endocrine organ involved in a multitude of functions necessary to maintain normal vessel function, including regulation of vascular tone, blood coagulation and thrombosis. Since the endothelium participates in these functions by secreting molecules that are pre-stored in their secretory vesicles, called WPBs, and given that only part of the molecules stored in these vesicles have been identified to date, previous research in our laboratory sought to identify new cargo molecules of WPBs. For this purpose, the lab used a proteomic analysis of the secreted proteins of WPBs after activation of endothelial cells, as shown as an illustration in Fig 1.14 (unpublished data of our lab).
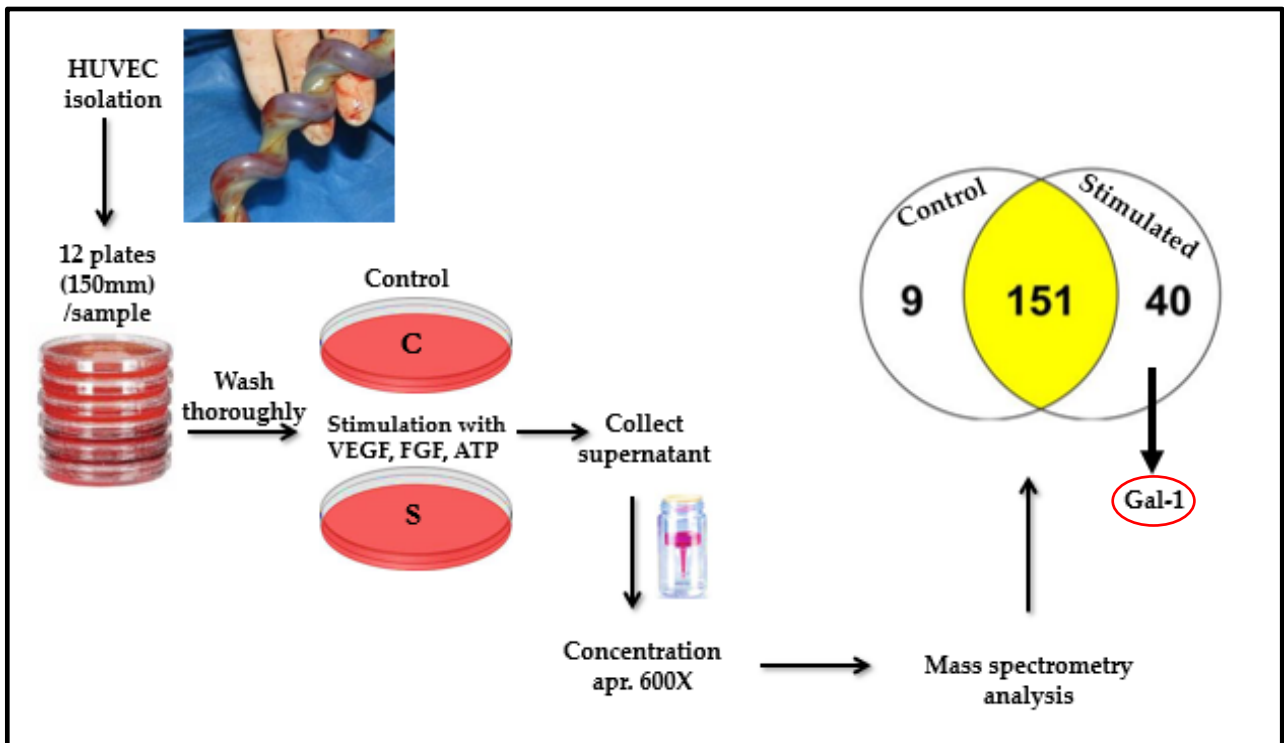
Figure 1.14- Schematic representation of the procedure followed for proteomic analysis in stimulated and unstimulated endothelial cells (HUVECs). *Large-scale HUVE cell culture, 12 plates (150mm), were activated with VEGF (50 ng/ml)/bFGF (15 ng/ml)/ATP (100 μM) for 1 h, to induce exocytosis of WPBs. The supernatant of the secreted proteins was collected, centrifuged and concentrated with filters and then analyzed by mass spectrometry (the process of producing peptides from the supernatant proteins, which were analyzed, is not shown). The same procedure was performed on HUVECs in which no induction was performed (control). The proteins identified were classified into those found in the stimulated only, control only and those found in both conditions, as shown in the Venn diagram. Among the identified new proteins, in the stimulated sample, was galectin-1 (Gal-1), as indicated in red. Unpublished data of our lab from previous research. Image created with BioRender.com.*

In the sample of activated cells, among the newly identified proteins was Galectin-1 (Gal-1), which, as described in section 1.5, is a protein known to be secreted unconventionally. This finding raised many questions as to whether this protein can indeed also use WPBs, vesicles of the conventional secretion pathway, for its secretion. So, immunofluorescence staining for endogenous Gal-1 and endogenous VWF (the main protein component of WPBs) was performed. As shown in Fig. 1.15, Gal-1 strikingly co-localizes with VWF in only a subpopulation of vesicles.
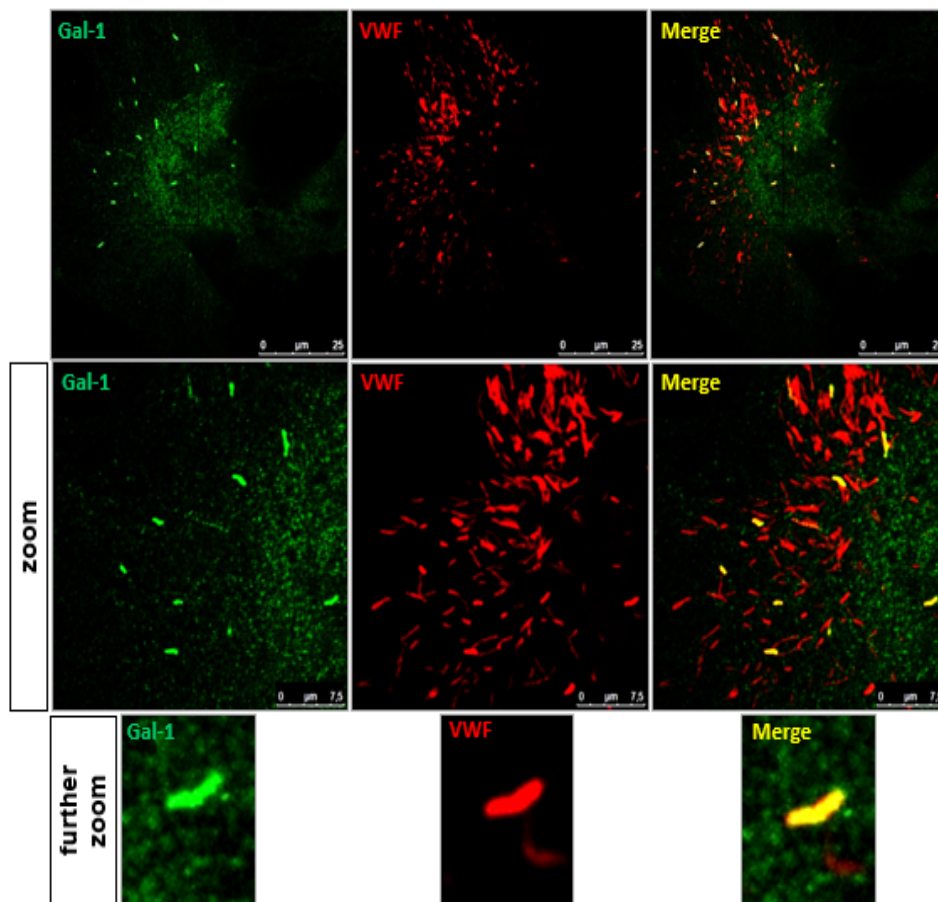
Figure 1.15- Gal-1 is localized in a subpopulation of WPBs in HUVECS. *Immunofluorescence of fixed HUVECs, stained for Gal-1 (green) and VWF (red) were analyzed by confocal microscopy. Gal-1 co-localizes with VWF in a subpopulation of rod-shaped WPBs. Unpublished data of our lab from previous research.*

1.7 Aim of the thesis

Previous research in our laboratory identified galectin-1 (Gal-1) to be localized in a subpopulation of the secretory vesicles, WPBs, as described in section 1.6. These findings were surprising since Gal-1 is a typical cytoplasmic protein known to be secreted unconventionally (escaping the classic ER-Golgi-PM secretory route), via an as to yet unknown mechanism. The finding that Gal-1 is present in WPBs, which are conventionally generated secretory vesicles (they originate from the Golgi, as a transport intermediate in the ER-Golgi-plasma membrane conventional secretory pathway), raises interesting questions about the mechanism that Gal-1 uses, an unconventionally secreted protein, to hijacks the conventional secretory pathway at its late stage, the secretory vesicles.

In the current master's thesis, **we approached two aspects of this theme:**

1. Given that Gal-1 is a cytoplasmic protein, the WPB-localized pool of this protein could be either present at the membrane, facing the cytosolic side of WPBs, or in their lumen. So, the first goal of the thesis was to **identify the exact topology of Gal-1 in WPBs, i.e. whether it is in the lumen or at the membrane surface of the vesicles.**

2. Since Gal-1 is localized in only some cells and in a sub-group of their WPBs, **we explored possible conditions that induce the entry of the protein into the vesicles**.

2. MATERIALS & METHODS

2.1 Antibodies

The antibodies used in this study are summarized in the tables below.

Primary antibodies						
Protein target	Host	Class/ Type	Conjugate	Company	Catalog number	Dilution
EGFP	alpaca	recombinant/ nanobody	ATTO 488	Proteintech	gba488	1:200
galectin-1	rabbit	polyclonal/ antibody	-	(production and purification in our laboratory)	-	1:100
Munc13-4	rabbit	polyclonal/ antibody	-	(production in Dr. H. Horiuchi laboratory)	-	1:200
von Willebrand factor	mouse	monoclonal/ antibody	-	Dako/Agilent	M0616	1:200
von Willebrand factor	rabbit	polyclonal/ antibody	-	Dako/Agilent	A0082	1:300

Table 2.1- Overview of the primary antibodies used in the study.

Secondary antibodies						
Species Reactivity	Host	Class	Conjugate	Company	Catalog number	Dilution
mouse	donkey	polyclonal	Alexa 594	Thermo Fisher Scientific	A21203	1:200
mouse	donkey	polyclonal	Alexa 680	Thermo Fisher Scientific	A10038	1:200
rabbit	donkey	polyclonal	Alexa 488	Thermo Fisher Scientific	A21206	1:200
rabbit	donkey	polyclonal	Alexa 594	Thermo Fisher Scientific	A21207	1:200

Table 2.2- Overview of the secondary antibodies used in the study.

2.2 Isolation of Human Umbilical Vein Endothelial Cells (HUVECs)

HUVE cells were isolated from the vein of healthy umbilical cords (kind donation by the Gynecology Clinic, University Hospital of Ioannina) using an established protocol of our laboratory.

Initially, the cord clots were surgically removed, and the umbilical cord vein was washed using a syringe with PBS (Phosphate Buffer Saline) solution. Subsequently, 3-way stopcocks were placed at both ends of the vein, i.e. inlet and outlet

along the cord, and were tied with surgical suture. The vein was washed with PBS. One end of the vein was then occluded, 0.1% collagenase solution (Collagenase type I, Worthington, LS004196) in PBS was inserted, the 3-way stopcock was again blocked, the cord was placed in a container containing PBS and incubated in a water bath at 37°C for 10 minutes.

To inactivate collagenase and collect cells, the cord was washed with 10 ml of enriched M199 (see section 2.3) followed by one wash with 10 ml of PBS and centrifugation for 10 minutes at 1000 rpm. The supernatant was discarded and the cell sediment was resuspended with an appropriate volume of Full M199, depending on the surface area of the plate to be cultured (usually resuspended with 3 ml for 1 well of 6-well plate). After 3hrs, so that the HUVECs had adhered to the plate, wash with PBS was performed. The cells were kept in the plate until their confluence reached 80-100%, so that the cells were ready for passaging.

2.3 Culture of HUVECs

HUVECs were cultured in M199 (PAN Biotech, P04-07500) enriched with 20% Fetal Bovine Serum (FBS) (Biosera, FB-1001B/500), 0.035 mg/ml ECGS (Endothelial Cell Growth Supplement) isolated from bovine brain (established isolation protocol in our laboratory), 0.05 IU heparin/ml (Merck, H3149 - 100KU), 1% L-glutamine (PAA Cell Culture Company, M11-004) and 1% penicillin/streptomycin (Thermo Fisher Scientific, Invitrogen, Antimycotic-Antibiotic, 15240062). In all experiments, cells were with passages between 1-4. Cells were handled in a laminar flow and class II safety cabinet and were maintained in an incubator in which the temperature was kept at 37°C, under humidified atmosphere containing 5% CO_2. Cells were grown in 6-well plates, 35mm or 100mm culture dishes, depending on the experiment, and for microscopy experiments in glass coverslips (round, 12 mm diameter, #1.5 (0.17 mm) thickness- Neuvitro, GG-12-1.5-oz) within 24-well plates or suitable microscopy plates (Ibidi, 81156 or 80806), previously incubated with rat type I collagen for at least 20 minutes at 37°C. All materials used were endotoxin-free.

2.4 Transfection of HUVECs with plasmid DNA

One day before transfection, 55,000 cells (counted with Neubauer chamber) were cultured on collagen-coated glass coverslips within a 24-well plate, so that the next day, i.e., the day of transfection, they were at an optical density of 50-60% coverage of the coverslip.

The transfection reagent used was METAFECTENE® PRO lipid (Biontex, T040-2.0), in a lipid to DNA ratio of 6:1. A mixture of lipid (3 µl) and plasmid DNA (0,5 µg) was incubated for 20 minutes at room temperature in unenriched M199 medium and the lipid/DNA mixture was added to cells in which the culture medium (enriched M199, see 2. 3) had been replaced with M199 medium supplemented only with 5 % FBS. Incubation for 3,5 hours followed. The cell growth medium was then replaced with enriched M199 medium (see section 2.3). 48 hours after transfection, the cells were fixed and the expression of the desired protein was checked with fluorescence microscopy.

2.4.1 Determination of transfection efficiency

Cells 48hrs after transfection, were fixed and after being permeabilized with 0.1% Triton X-100 (see section 2.8) were incubated with GBP nanobody (conjugated with ATTO 488) to enhance the signal of EGFP or EGFP-Rab27a protein, depending on the plasmid used. Immunofluorescence staining for VWF, a protein expressed in all cells, transfected and non-transfected, was also performed. On confocal microscope (Leica TCS SP5 Confocal microscope) and using 40X lens, in at least 10 random fields per case, the number of transfected cells was counted and compared with the total number of cells (transfected and non-transfected). By appropriate reduction, the percentage of transfected cells per condition was calculated.

2.5 Plasmid DNA production and purification

The desired plasmids used, pEGFP-C1 and pEGFP-C1-Rab27a, were ready-made by previous members of the laboratory (see Figure 2.1, plasmid map). For this research, we replicated the plasmids in DH10B strain of E. Coli (after transfection) and performed plasmid purification.
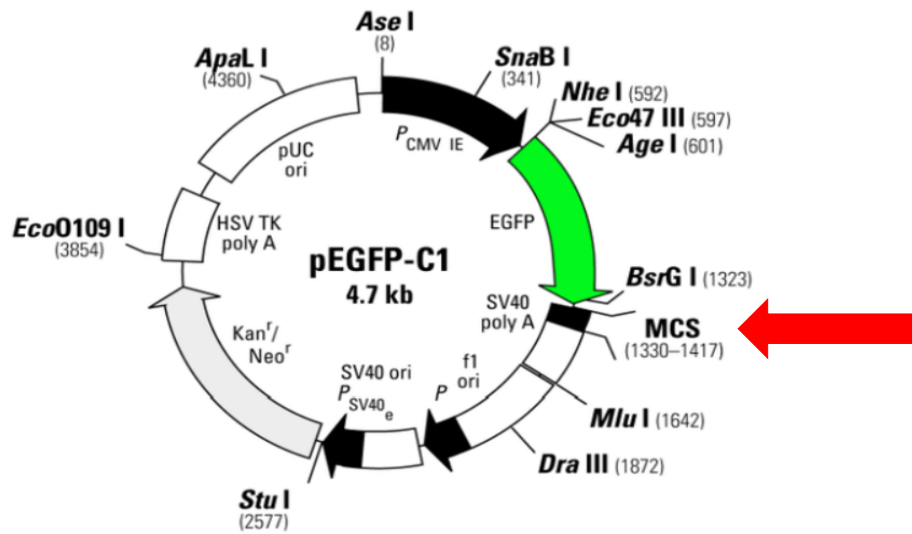
Figure 2.1 - Map for pEGFP-C1. The red arrow shows the region where the gene for Rab27a was inserted into the multiple cloning site (MCS), after restriction digestion with EcoRI and XhoI enzymes.

2.5.1 Bacterial transformation

The transformation was done by the "thermal shock" method. Specifically, the bacteria (E. coli strain DH10B) were transferred from -80°C (where they are stored) to ice until they thaw. Then 100ng-1μg of plasmid (optimally 400ng for pEGFP-C1-Rab27a plasmid and 800ng for pEGFP-C1 plasmid) were added to 100μl of bacterial solution, followed by gently stirring the solution by hand. This was followed by incubation on ice for 30 minutes. The sample was then incubated at 42°C (in a water bath) for 30 seconds and transferred to ice for 2 minutes. This was followed by introduction of 500 μl LB [Luria Broth - 1% w/v NaCl (Lach- Ner), 1% w/v Tryptone or Casein (NEOGEN), 0.5% Yeast Extract (NEOGEN)] under sterile conditions and incubation at 37°C, under agitation (200 rpm), for 1 hour.

Then, bacteria were cultured in two LB-Agar (with 50μg/ml Kanamycin) petri plates, as follows: for the first, 50μl from the previous solution were transferred and plated, and for the second, the solution was first centrifuged at 6000 rpm for 2 minutes, the supernatant was discarded all but 100μl, the bacteria were resuspended in this

volume and then plated on the dish. Finally followed by overnight incubation at 37°C, with the dishes placed inverted and in an incubator under humidified atmosphere, for the transformed bacteria to proliferate.

2.5.2 Creation of 100ml liquid bacterial culture

To produce the plasmids in the desired quantities, we made bacterial cultures of total volume of 100ml, which were done with an intermediate pre-culture of 5ml volume.

1) Pre-culture of 5 ml: 5 ml of LB (with 50μg/ml Kanamycin) were added to a sterile falcon tube under sterile conditions. Then with a pipette tip, a colony of transformed bacteria was transferred in the tube and incubated at 37°C, for 6 hours, under agitation (200rpm).

2) Culture of 100 ml: 1.5 ml, under sterile conditions, from the 5 ml pre-culture were transferred to a conical flask containing 100 ml of LB (with 50μg/ml Kanamycin) and incubated at 37°C, overnight, under agitation (200rpm).

2.5.3 Extraction and purification of plasmid DNA

To extract the plasmid of interest, GenElute™ Endotoxin-free Plasmid Midiprep Kit (Sigma, PLED35-1KT) was used, following the procedure in the User Guide that accompanies the product.

Finally, in the plasmid solution, the concentration was calculated, and the purity was checked with A260/A280 and A260/230 ratios, using NanoDrop Microvolume Spectrophotometer (Thermo Fisher Scientific).

2.6 Alkalinization of the intra-WPB pH of HUVECs using NH$_4$Cl solution

First, an ammonium chloride (NH$_4$Cl) solution of 150mM concentration in ddH$_2$O was prepared, the pH of which was adjusted to 7.4 (equal to the pH of the culture medium of HUVECs) and then sterilized using a syringe filter of pore size: 0.2μm (Sarstedt, 83.1826.001).

Appropriate volume of the solution (27ml for 100ml final volume solution) was transferred to appropriate volume (73ml for 100ml final volume solution) of enriched

M199 medium (see section 2.3) but which had 25% FBS instead of 20%, to achieve a final NH_4Cl solution concentration of 40mM. Thus, in the final solution the concentration of NH_4Cl was 40mM, FBS was 20% and the other components of the enriched M199 (apart from FBS) were reduced, with the total osmolarity of the solution being 300mM (equal to the HUVEC culture medium).

HUVECS were incubated for 4 hours with the above 40mM NH_4Cl solution, followed by fixation and immunofluorescence staining for the proteins under study (see section 2.8).

2.7 Confluence experiment

HUVECs from culture plate (usually one well from 6-well plate) were split at a ratio of 1:2 (considering the difference in surface area) to four ibidi 35mm dishes (Ibidi, 81156), previously incubated with rat type I collagen, so that the next day the cells had 100% confluence. One dish per day, consecutively for four days in total were isolated and cells were fixed. After the four days, all four dishes were immunofluorescently stained for endogenous Gal-1 and VWF proteins. Cells were studied in the SP5 Laser Confocal Microscope. To facilitate cell counting, each field (zoom 1) was subdivided into four subfields (zoom 1.98), which were captured. When calculating the percentage of cells that had Gal-1 positive WPBs, in the total number of cells, those that did not have VWF (and thus WPBs) were not counted since were cells that had lost their endothelial phenotype.

2. 8 Migration assay

HUVECs were cultured on glass coverslips (four different coverslips corresponding to different fixation times within 24 hours), within 24-well plates, previously incubated with rat type I collagen for at least 20 minutes at 37ºC, and were allowed to form a confluent monolayer. Then, in each coverslip, a yellow tip was used to scratch and remove cells from a discrete area of the confluent monolayer to form a cell-free zone into which cells at the edges of the wound can migrate. Coverslips were fixed at 0, 6, 12 and 24 hours after scratching, were immunofluorescently stained for endogenous Gal-1 and VWF proteins and were studied in the SP5 Laser Confocal Microscope.

2.9 Indirect immunofluorescence

HUVECs were cultured on glass coverslips within 24-well plates or suitable microscopy plates (Ibidi, 81156 or 80806), previously incubated with rat type I collagen for at least 20 minutes at 37^0C. After the end of each experiment, first three washes were performed with PBS (1X)-$MgCl_2$(1mM)-$CaCl_2$ (1mM) solution and then the cells were incubated with 4% paraformaldehyde (PFA) solution in PBS for 20 min at room temperature (RT), which induces fixation. Then three washes with PBS (1X) solution were performed, followed by incubation with 50 mM NH_4Cl in PBS (1X) solution for 30 min at RT, for quenching the free aldehyde groups of PFA. After three washes with PBS (1X), cells were incubated with 0.1% Triton X-100 in PBS (1X) solution for 10 minutes at RT, to achieve membrane permeability, allowing penetration of antibodies and detection of intracellular proteins. After three washes with PBS (1X), cells were incubated with blocking solution (10 % FCS in PBS) for 60 minutes at RT. Cells were then incubated for 1 hour at RT (or overnight at 4^oC for Munc13-4 protein detection) with primary antibody solution diluted in blocking solution (for dilution for each antibody used, see Table 2.1). This was followed by three washes with PBS (1X) solution and cells were incubated with secondary antibodies conjugated with Alexa fluorochromes (Alexa 488, 594, 680) diluted in blocking solution (see Table 2.2) for 40 minutes, at RT, in the dark. Next three washes with PBS (1X) solution were performed. Glass coverslips were mounted on microscope slides with Mowiol solution (Sigma, 81381) which contained 100 mg/ml DABCO (Sigma, D27802), and were allowed to dry at RT overnight. For ibidi plates, ibidi Mounting Medium (Ibidi, 50001) was used. Samples were observed under a confocal laser scanning microscope (Leica TCS SP5 Confocal microscope).

2.10 Laser Scanning Confocal Microscopy

Cells after immunofluorescence staining were studied using Leica TCS SP5 Confocal microscope and Las AF software. The scanning frequency was performed at 400 Hz and an image resolution of 512x512 pixels was used. Specimens were observed with a Leica 63x 1.4 NA 1.4 NA oil UV lens and pinhole of size 1 Airy Units (AU), unless otherwise noted.

2.11 Statistical analysis

For the confluence experiment, statistical analysis was performed using GraphPad Prism 10.1.0 (316) software (Graph-Pad Software, San Diego California, USA). Data were obtained from three independent replicates of the experiment and were presented in the graph, calculating the standard deviation (SD) of the values. Data were analyzed by standard one-way ANOVA followed by Bonferroni for multiple comparisons.

3. RESULTS

3.1 Galectin-1 co-localizes with the main cargo of WPBs, VWF, in a small subset of WPBs and in a sub-population of cells

Previous work in the lab showed that Gal-1 is present in a subpopulation of the secretory vesicles WPBs, in a group of cells, the percentage of which varied among different HUVEC preparations. As these findings were somewhat puzzling, we first sought to confirm that Gal-1 is indeed localized at WPBs. As shown in Figure 3.1, using immunocytochemistry and confocal microscopy, we confirmed that Gal-1 is localized at WPBs, in addition to the nucleus and cytoplasm that has been reported in the literature. The identity of these organelles as WPBs was based on the staining of VWF, the major cargo molecule of WPBs (Figure 3.1). We also observed that Gal-1 is localized only in a subpopulation of WPBs. Interestingly the two proteins (Gal-1 and the marker VWF) often times were found to co-localize in bended-shaped WPBs (see white arrow in Figure 3.1), which could possibly arise from a homotypic fusion of two straight-lined WPBs. Notably, these data are based on endogenous proteins, while the specificity of the antibodies has been evaluated by competition and siRNA-based approaches.

Independently of the exact origin of the subpopulation of the Gal-1-positive WPBs, the above experiments assured us that our working conditions allow us to reproduce the identification of Gal-1 at WPBs in freshly isolated HUVECs.
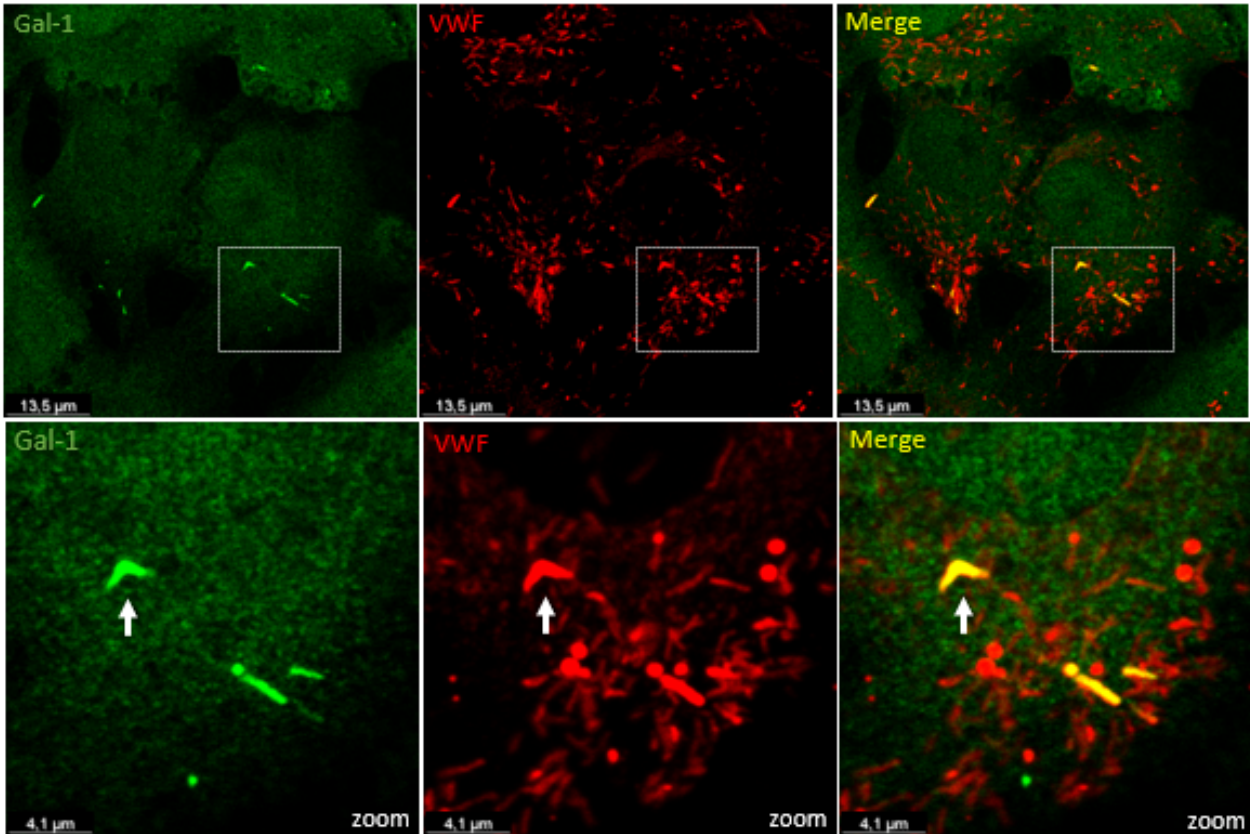
Figure 3.1- Galectin-1 is localized in a subset of WPBs in HUVECs. *Immunofluorescence of fixed HUVECs, stained for Gal-1 (green) and VWF (red) were analyzed by confocal microscopy. It appears that Gal-1 co-localizes with VWF in rod-shaped WPBs as well as in a bended WPB (white arrow), possibly arising from the homotypic fusion of two distinct WPBs.*

Intriguingly, in several preparations of the freshly isolated HUVECs, we observed Gal-1 positive WPBs in only a few cells per field of view. For example, as shown in Figure 3.2 (upper part), only one cell shows localization of Gal-1 in a typical WPB. Besides, we also observed that the number of cells that contained Gal-1 positive WPBs varied among different HUVEC preparations. As the observation of the large heterogeneity in the number of Gal-1 positive cells per field of view, and the heterogeneity in Gal-1 positive WPBs per cell is very intriguing, in the present study we sought to investigate the responsible conditions that drive these effects (in section 3.8). Yet, before addressing this issue, it was important to first investigate the exact topology of Gal-1 in WPBs.
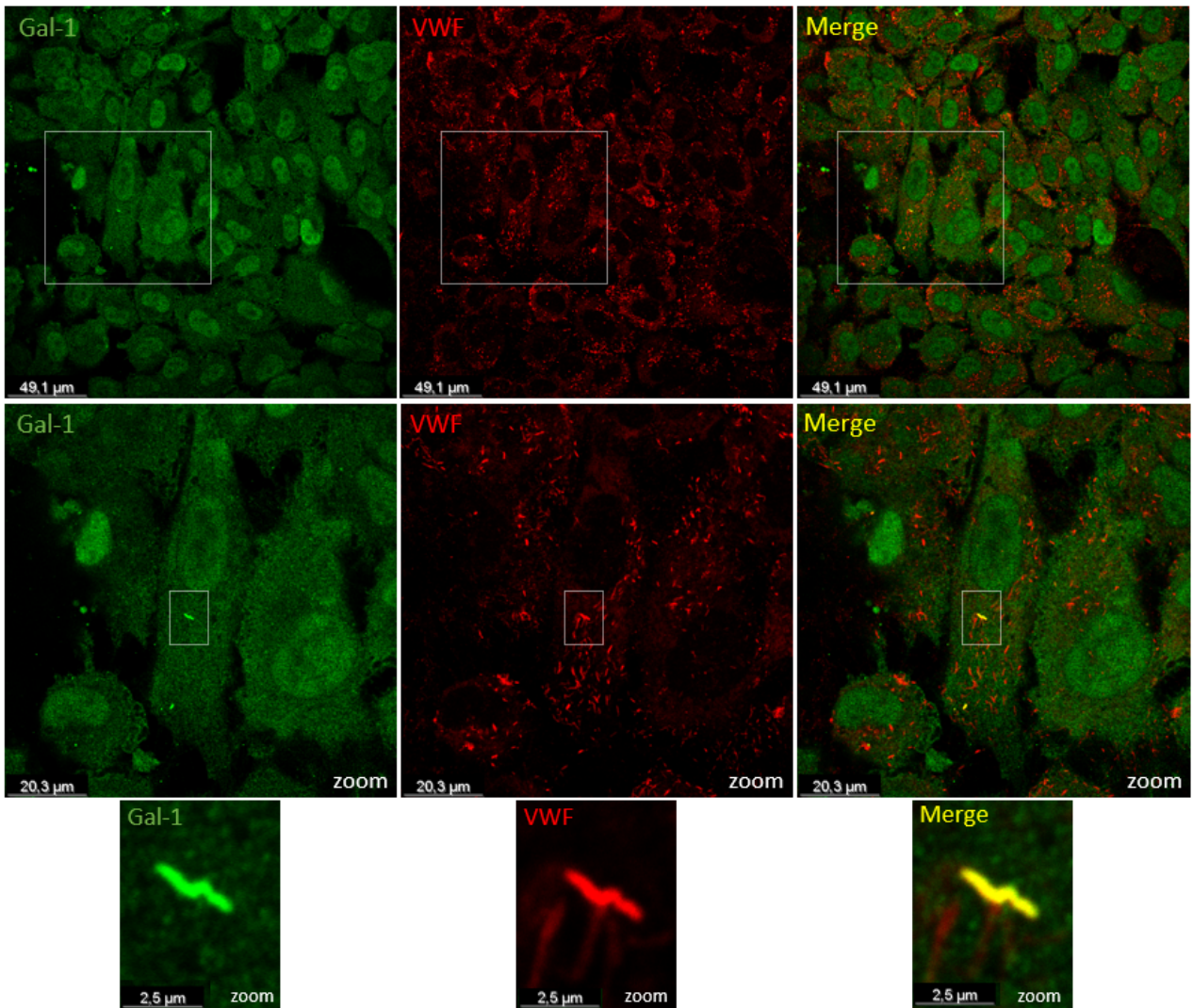
Figure 3.2- Galectin-1 is usually localized in WPBs in a very small number of cells per field, in untreated cells.
Immunofluorescence of fixed HUVECs, stained for Gal-1 (green) and VWF (red) and observation by confocal microscopy. In the field, only one cell has Gal-1 positive WPBs, which is shown in magnification in the middle part of the figure. In the lower part, a WPB generated by homotypic fusion of WPBs is shown, which is positive for Gal-1.

3.2 The challenges inherent in the confocal microscopy resolution

Given that Gal-1 is a known cytoplasmic protein that lacks a signal sequence, its localization in WPBs raises intriguing questions. At first, since this protein is synthesized in the cytoplasm, its presence at WPBs could be either explained by a simple docking at the cytoplasmic surface of WPBs, thus becoming a peripheral membrane protein facing the cytoplasm, or by a more intricate mechanism that may involve transport of the protein through the membrane, thus becoming a lumenal cargo. Distinguishing between these two possibilities (peripheral versus lumenal) is critical, since it has different implications on the role of the protein and on its subsequent fate. Thus, we first sought to address the exact localization of Gal-1 at WPBs (membrane peripheral versus lumenal). However, as explained below, this is not a task that can be resolved by confocal microscopy. Due to the exceptionally diminutive diameter of the vesicles, confocal microscopy which can reach 500 nm in axial resolution under optimal conditions (Fouquet et al., 2015), is unable to separate the periphery from the lumen of the vesicle, since this distance is lower than the optical resolution of the microscope (500nm). Thus, as shown schematically in Figure 3.3, when a lumenal protein (e.g. VWF) and a membrane protein (e.g. Rab27a) are studied in WPBs, confocal microscopy shows complete co-localization of these, which is not actually the case (refer to Figure 3.4 for confocal images depicting the study of VWF and Rab27a proteins within WPBs). Therefore, although Figures 3.1 and 3.2 show complete co-localization of Gal-1 and VWF proteins, this does not necessarily mean that Gal-1 is a lumenal protein. Also, considering that Gal-1 is a cytoplasmic protein, it could possibly accumulate on the membrane towards the cytoplasmic side of the vesicle. For this reason, the first aim of this study was to investigate the exact topology of Gal-1 in the WPBs.
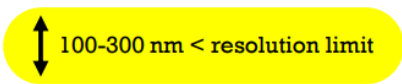
Confocal microscopy	Schematic drawing of a membrane and a lumenal marker of a WPB
Membrane protein Lumenal protein · 100-300 nm < resolution limit	Membrane protein Lumenal protein

Figure 3.3- Schematic depiction of challenges encountered in confocal microscopy analysis while studying WPBs vesicles. The left panel shows in cartoon the image obtained when studying with confocal microscopy a membrane protein (green) and a lumenal protein (red) in WPBs vesicles, i.e., complete co-localization of these is observed since the vesicle diameter is smaller than the resolution limit of the microscopy. The right part of the image shows, in cartoon, the image that would be obtained if there was no resolution issue, i.e., the membrane protein would appear in the periphery while the lumenal protein inside the vesicle.

3.3 Extraction and purification of pEGFP-C1 and pEGFP-C1-Rab27a plasmids

To determine the topology of Gal-1 in WPBs, we needed a marker of the WPB membrane, i.e. a protein that is only found in the membrane and not in the lumen of the vesicle. We chose Rab27a, a protein that is recruited to the periphery of the vesicle during maturation of WPBs (see introduction). As the endogenous protein was not apparent with our available tools and with standard immunofluorescence procedure (primary and secondary antibody), we overexpressed the protein by transfection.

The first step was to perform plasmid production in DH10B strain of E. Coli and purification with kit for Endotoxin-free plasmid midiprep (see section 2.5). We performed the procedure first for the pEGFP-C1 vector without the insert (EGFP protein expression), which was used to optimize the transfection protocol, and then for the pEGFP-C1- Rab27a plasmid containing the insert (Rab27a gene), from which the desired recombinant EGFP-Rab27a protein will be expressed after transfection.

After extraction and purification, the concentration and the purity of plasmids were estimated. As shown in Table 3.1, both plasmids showed ratios of absorbance at 260 and 280 nm between 1.7 - 2.0 and therefore are considered pure. Also, the 260/230 ratio, used as a secondary measure of DNA purity, was between the desired range of 2.0 and 2.2, for both plasmids. The above indicated that we could proceed to the next stage, namely the optimization of the transfection protocol.

Plasmid	pEGFP-C1	pEGFP-C1- Rab27a
Concentration	0,571 µgr/ µl	0,504 µgr/µl
A260/280	1,93	1,92
A260/230	2,08	2,09

Table 3.1- Concentration and purity of the extracted plasmids. *The pEGFP-C1 plasmid has the EGFP orf and the pEGFP-C1-Rab27a additionally has the Rab27a orf, fused to the EGFP orf (see map on Figure 2.1). The values in the table are the means of two consecutive measurements, using NanoDrop Microvolume Spectrophotometer (Thermo Fisher Scientific).*

3.4 Optimisation of transfection efficiency

For the transfection we chose a non-viral lipid-based protocol, using the reagent METAFECTENE® PRO (Biontex) as lipid. As transfection is a stressful process for the cells and the efficiency can vary significantly depending on the conditions chosen, we first optimized our conditions. For this, in a first step we used the pEGFP-C1 vector expressing only the EGFP protein, which is expressed at high levels and allows easy separation of transfected from non-transfected cells and therefore determination of transfection efficiency, since transfected cells fluoresce strongly after appropriate stimulation under a fluorescence microscope (EGFP: Excitation max: 488, Emission max: 509). We tested different conditions by introducing different amounts of DNA and lipid, achieving varying ratios. For the different conditions, we determined the confluency rate of the cells 48hrs post-transfection, i.e. the time before cell fixation, and the transfection efficiency, as shown in Table 3.2. We note that the optimal transfection efficiency (40%) was achieved when 0.5µg DNA and 3µl lipid were added (DNA/lipid ratio: 1:6).

pEGFP-C1 plasmid				
µg DNA	µl lipid	ratio (DNA/lipid)	% cell confluency (48hrs post-transfection)	% transfection efficiency
0,5	1,5	1:3	50	35
0,5	3	1:6	70	40
0,5	7	1:14	80	10
1	1	1:1	90	10
1	3	1:3	10	30
1	7	1:7	30	30

Table 3.2- The different combinations of DNA (pEGFP-C1 plasmid) and lipid (METAFECTENE® PRO) amounts tested, cell viability (% cell confluency) and transfection efficiency are presented. *The optimal combination is marked in green.*

To verify the optimal transfection conditions, we repeated the assay this time for the plasmid of interest, namely pEGFP-C1-Rab27a, as differences in transfection efficiency are possible when different plasmids are used. As shown in Table 3.3, the confluency and transfection efficiency rates are similar to the case of pEGFP-C1 and the optimal condition is also achieved when 0.5µg DNA and 3µl lipid are added (DNA/lipid ratio: 1:6).

pEGFP-C1-Rab27a plasmid				
µg DNA	µl lipid	ratio (DNA/lipid)	% cell confluency (48hrs post-transfection)	% transfection efficiency
0,5	1,5	1:3	30	30
0,5	3	1:6	90	50
0,5	7	1:14	80	<5
1	1	1:1	90	<10
1	3	1:3	10	40
1	7	1:7	70	30

Table 3.3- The different combinations of DNA (pEGFP-C1-Rab27a plasmid) and lipid (METAFECTENE® PRO) amounts tested, cell viability (% cell confluency) and transfection efficiency are presented. *The optimal combination is marked in green.*

Figure 3.4 shows an EGFP-Rab27a transfected cell, which has been immunofluorescence stained for VWF as well. We observe that Rab27a indeed co-localizes with VWF, in rod-shaped WPBs. We also notice that, as analysed above, confocal microscopy is unable to resolve the lumen (where VWF is located) from the membrane of the vesicle (where Rab27a is located), given that its resolution limit (500 nm) is above the WPB diameter (<300 nm). If the resolution of the microscope was sufficient, we would observe Rab27a only in the periphery of the WPB, leaving the interior blank (lumen), which is not the case in this image.
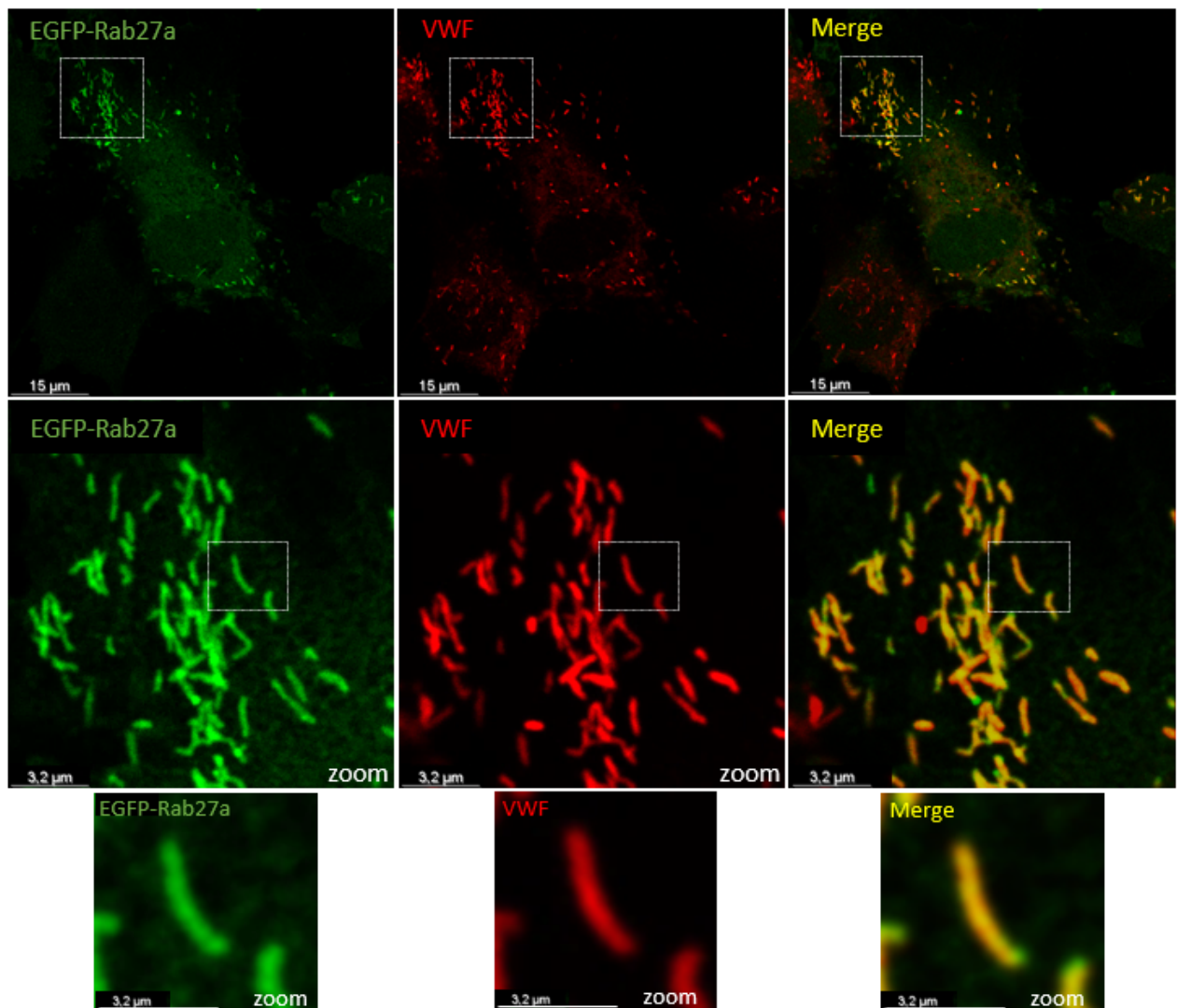

Figure 3.4- Transfected cell for EGFP-Rab27a (green), in which immunofluorescence staining for endogenous VWF (red) was performed. *We observe that Rab27a is co-localized with VWF in WPBs. We also notice that confocal microscope analysis is not sufficient to distinguish the lumen (containing VWF) from the membrane (containing Rab27a) in the vesicles.*

3.5 Increasing WPBs' diameter using NH$_4$Cl solution

In order to circumvent the obstacle imposed by the resolution limitation of confocal microscopy, and to separate the lumen from the periphery of the WPBs, we changed the shape of the vesicles, from elongated to rounded, after incubating the cells with ammonium chloride (NH$_4$Cl) solution, as shown schematically in Figure 3.5. More specifically, exposure of cells to the weak base NH$_4$Cl increases intra-WPB pH from ~5.5 to >7.4 and gradually causes the WPB morphology to change from elongated to rounded. The rounding of WPBs leads to a significant increase in their diameter and thus confocal microscopy resolution is sufficient to distinguish the lumen from the periphery of the vesicle.
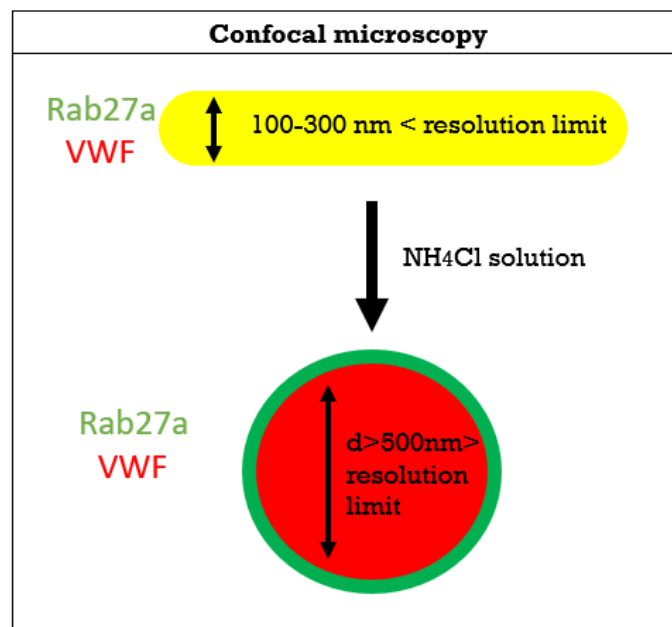
Figure 3.5- Cartoon representation of the change in the shape of WPBs, after incubating HUVECs with ammonium chloride (NH$_4$Cl) solution, allowing separation of the membrane from the vesicle lumen, by confocal microscopy. *Rab27a is a membrane protein while VWF is a lumenal protein.*

Although the use of NH$_4$Cl for WPB rounding has been reported before, there is ambiguity as to the required cell incubation time, ranging from minutes to hours (Erent et al., 2007; Kiskin et al., 2010, p. 201, 2014). Therefore, we initially tested three different incubation times, i.e., 2, 3 and 4 hours. As shown in Figure 3.6, already after 2 hours of incubation with NH$_4$Cl (of final concentration 40mM in M199) many WPBs had become rounded in the cells, but also several elongated ones remained, whereas

after 3 or 4 hours of incubation, almost all WPBs had become rounded. It should be noted that there were differences between cells in each condition, with some showing more and others less rounded WPBs, but in general the pattern shown in Figure 3.6 was followed. For our experiments, we chose to incubate the cells for 4 hours with the NH_4Cl solution.
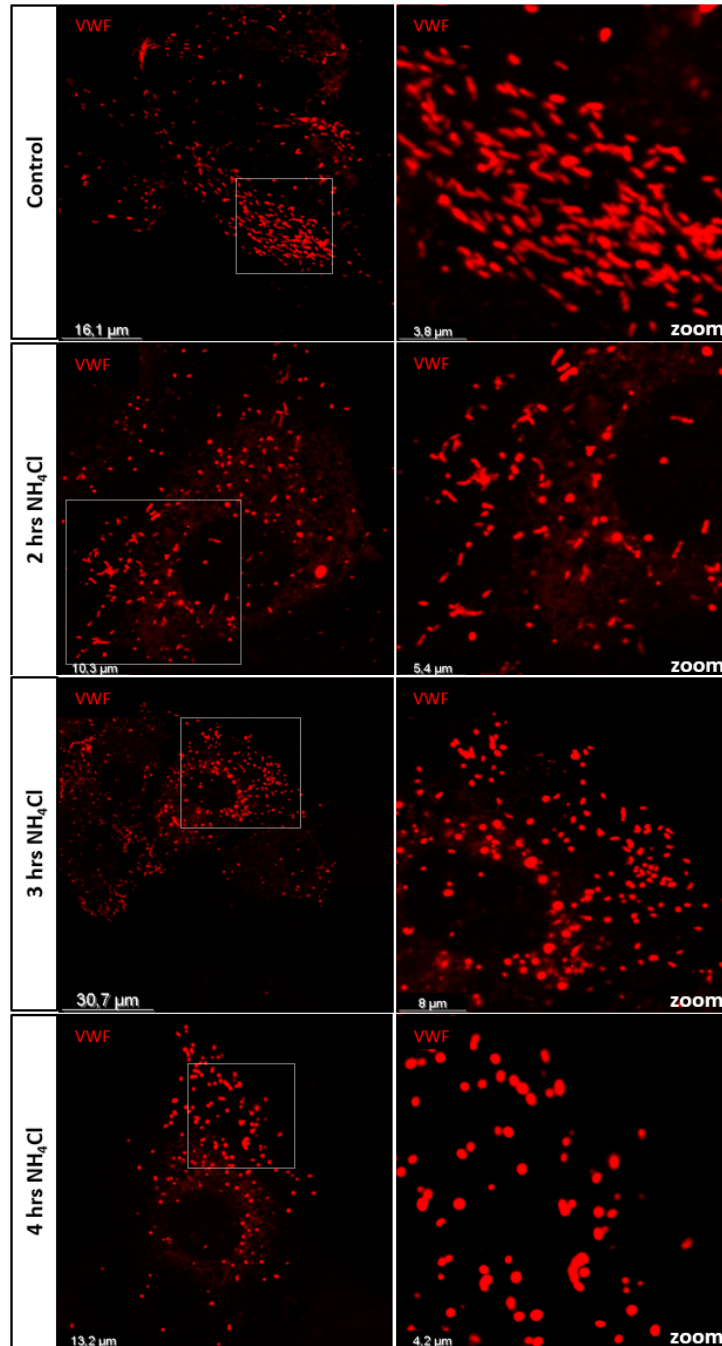
Figure 3.6 - Incubation of HUVECS with NH_4Cl changes the morphology of WPBs, from elongated to rounded.
Cells were incubated for 2 hrs, 3 hrs, 4 hrs or not incubated at all (Control) with NH_4Cl solution of final concentration 40mM in Medium 199 (M199), followed by fixation, immunofluorescence for VWF (red) and observation by confocal microcopy. We observe that after 2 hrs several elongated WPBs are left while after 3 or 4 hrs of incubation, most WPBs have become rounded.

3.6 Study of membrane markers on rounded WPBs

Since we found the conditions to induce the rounding of WPBs, which increases their diameter, we wanted to test whether confocal microscopy resolution could under these conditions separate the lumen from the periphery of the vesicle. For this purpose, we compared the topology of VWF, located in the lumen, with two different proteins: Rab27a and Munc13-4 (an effector of Rab27a (Zografou et al., 2012)), both known to be located in the periphery of the vesicle (see introduction). Rab27a was overexpressed by transient transfection, while for Munc13-4 the endogenous protein was studied. If microscopy resolution is sufficient, we should be able to distinguish in the rounded WPB a "ring", formed by the membrane protein in the periphery of the vesicle, with VWF located inside this "ring".

3.6.1 Rab27a as membrane marker

HUVEC cells were transfected with the pEGFP-C1- Rab27a plasmid, which leads to overexpression of EGFP-Rab27a protein, and the cells were incubated for 4hrs with NH_4Cl solution, to make the WPBs rounded, before fixation. As shown in Fig. 3.7, in the rounded WPBs Rab27a indeed forms a ring at the periphery of the vesicle while VWF is present in the center. This means that, under these conditions, microscopy resolution is sufficient to distinguish the lumen from the WPB membrane and therefore to investigate the topology of Gal-1 in WPBs, which is one of the main aims of the thesis. However, for confirmation, we also checked with another marker of the vesicle membrane, the Munc13-4 protein.
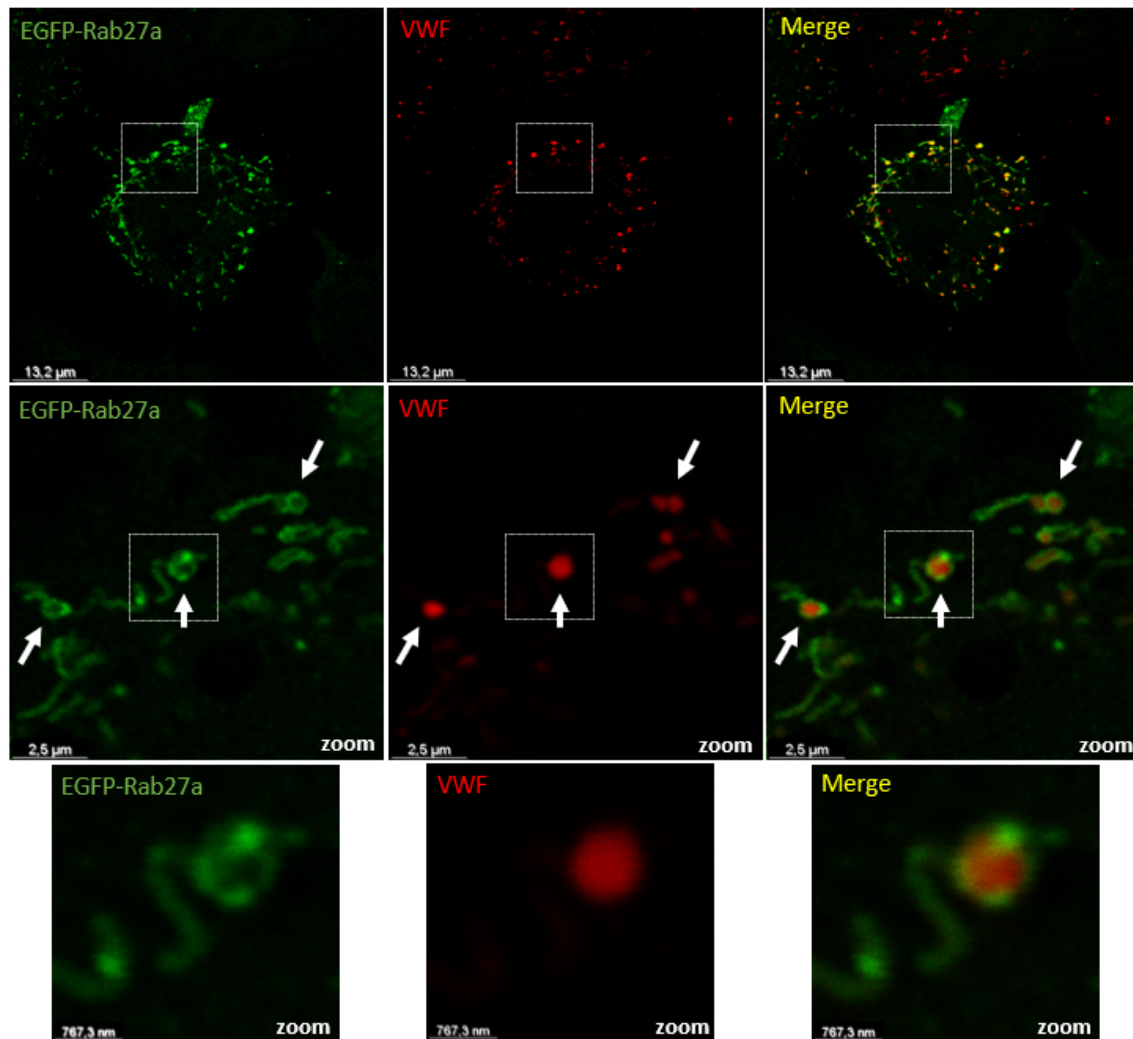
Figure 3.7- In rounded WPBs it is possible to separate the membrane from the lumen by confocal microscopy. *Transfected HUVECs that overexpress EGFP-Rab27a, were incubated for 4 hrs with NH₄Cl solution at a final concentration of 40mM in M199, followed by fixation, immunofluorescence for endogenous VWF (red) and Rab27a (green) and observation by confocal microcopy. We note that Rab27a, a protein located outside the vesicle towards the cytoplasm, appears to form a ring and is therefore a marker of the vesicle periphery. In contrast, VWF, which is the main cargo of WPBs and is located inside them, appears to be located inside the ring and is therefore a marker of the lumen of the vesicle.*

3.6.2 Munc13-4 as membrane marker

As shown in Figure 3.8, in the rounded WPBs we observe that Munc13-4 is located in the periphery of the vesicle with VWF being in the center of it, after immunofluorescence staining. This is another confirmation that our chosen conditions are sufficient to separate the lumen (where VWF is located) from the membrane (where Munc13-4 is located) of the vesicle. In this case both proteins (Munc13-4 and VWF) were studied in their endogenous form and levels.
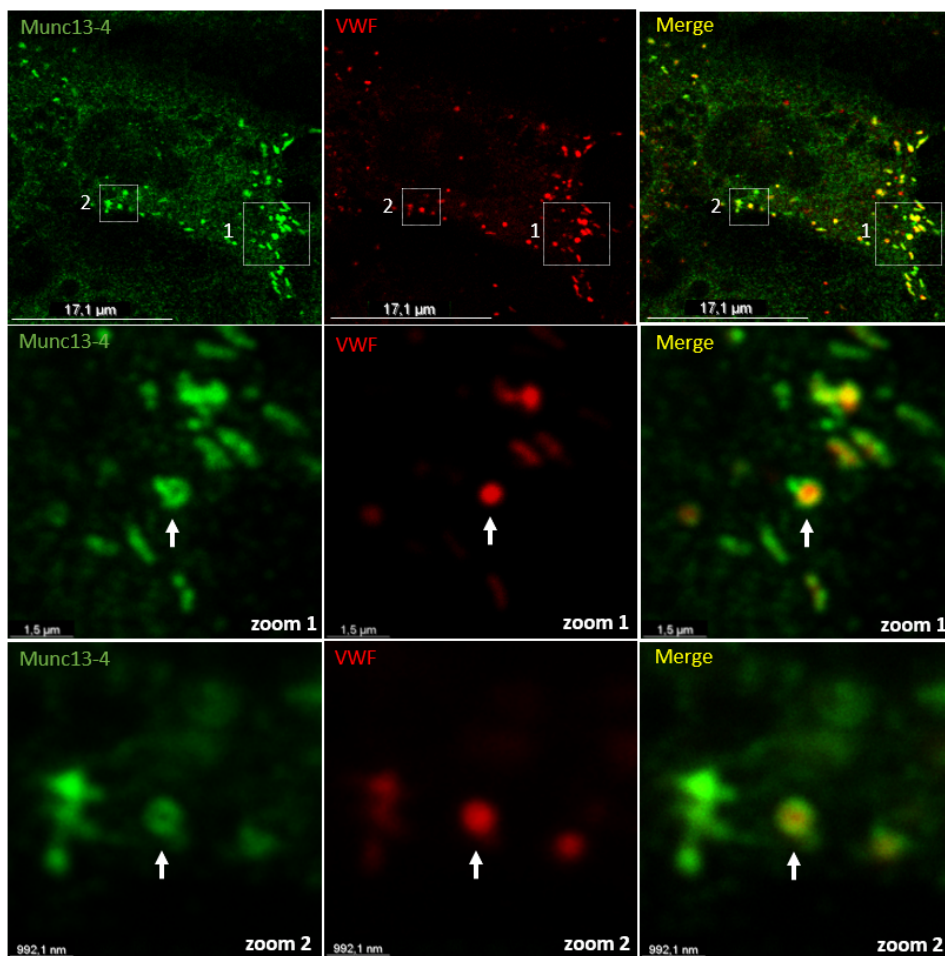
Figure 3.8- Confirmation that confocal microscopy can separate the membrane from the lumen in rounded WPBs. *HUVECs were incubated for 4 hrs with NH₄Cl solution at a final concentration of 40mM in M199, followed by fixation, immunofluorescence for the endogenous proteins: VWF (red) and Munc13-4 (green) and observation by confocal microcopy. We note that Munc13-4, a protein located outside the vesicle towards the cytoplasm, appears to form a ring and is therefore a marker of the vesicle periphery. In contrast, VWF, which is the main cargo of WPBs and is located inside them, appears to be located inside the ring and is therefore a marker of the lumen of the vesicle.*

3.7 Galectin-1 is located in the lumen of WPBs

Given that both Rab27a and Munc13-4 in the rounded WPBs showed the same pattern (ring around VWF, see Figures 3.7 and 3.8), it means that both proteins are equally appropriate as peripheral markers and therefore that we could use either of them for experiments to find the topology of Gal-1. However, since the primary antibody available in our laboratory for the Mun13-4 protein is from a rabbit host, the same host as that of Gal-1 antibody, we preferred to work with Rab27a in transfected cells. In this case (as described in 2.1 section) the primary antibody for VWF was in a mouse host, the primary antibody for Gal-1 was in a rabbit host and for overexpressed EGFP-Rab27a we used for additional amplification GFP binding protein (GBP nanobody) from alpaca host.

To find the exact topology of Gal-1 in the WPBs, i.e. whether it is in the lumen or around the vesicles, we performed triple immunofluorescence staining for Gal-1, VWF and Rab27a proteins. The two possible scenarios are as follows: that Gal-1 co-localizes with VWF, and that Rab27a is located as a ring around, which would imply that Gal-1 enters the lumen of the vesicle. In contrast, in the case where Gal-1 co-localizes with Rab27a and is in the form of a ring, with VWF lying inside, this would mean that Gal-1 is at the membrane, facing the cytosolic side of WPBs.

Interestingly, we found that Gal-1 is located in the lumen of the WPB. Some examples where the topology of Gal-1 is shown are the Figures 3.9 and 3.10. In particular, in Figure 3.10 (middle and bottom parts) are shown two adjacent rounded WPBs that both contain VWF in the center and Rab27a in the periphery, but only one is Gal-1 positive. These data suggest that Gal-1 is found only in a subpopulation of WPBs, and that the red staining (for Gal-1 protein) is not an artifact, since it is only found in a subset of WPBs.
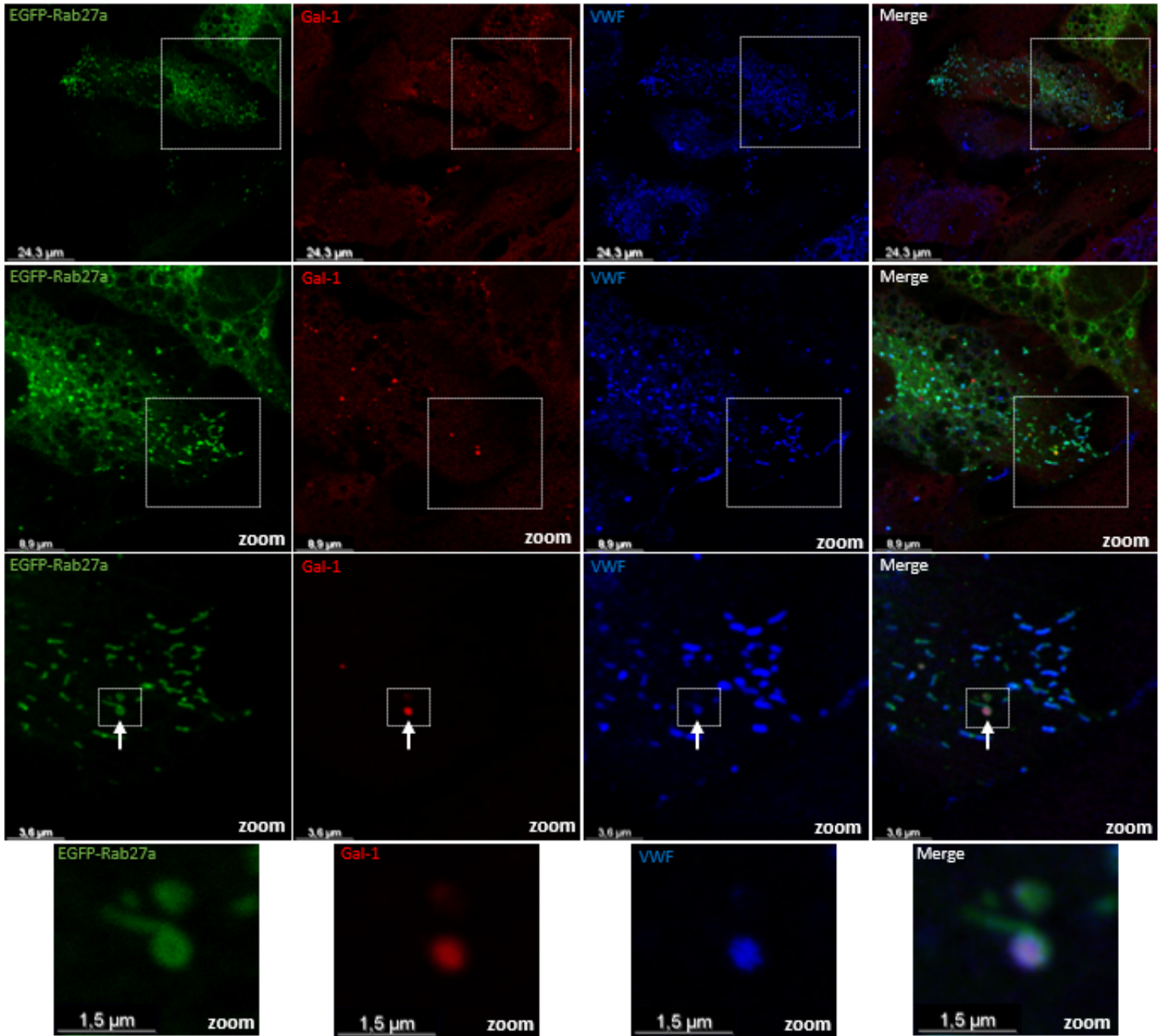
Figure 3.9- Galectin-1 is stored in the lumen of WPBs. *Triple immunofluorescence staining for EGRP-Rab27a (green), Gal-1 (red) and VWF (blue) in fixed HUVECS and observation by confocal microcopy. Gal-1 co-localizes with VWF inside the vesicle, with Rab27a surrounding the rounded WPB. The first two sets of images were captured with pinhole of size 1 Airy Unit (AU) whereas the last two sets of images were captured with a 0.6 AU pinhole.*
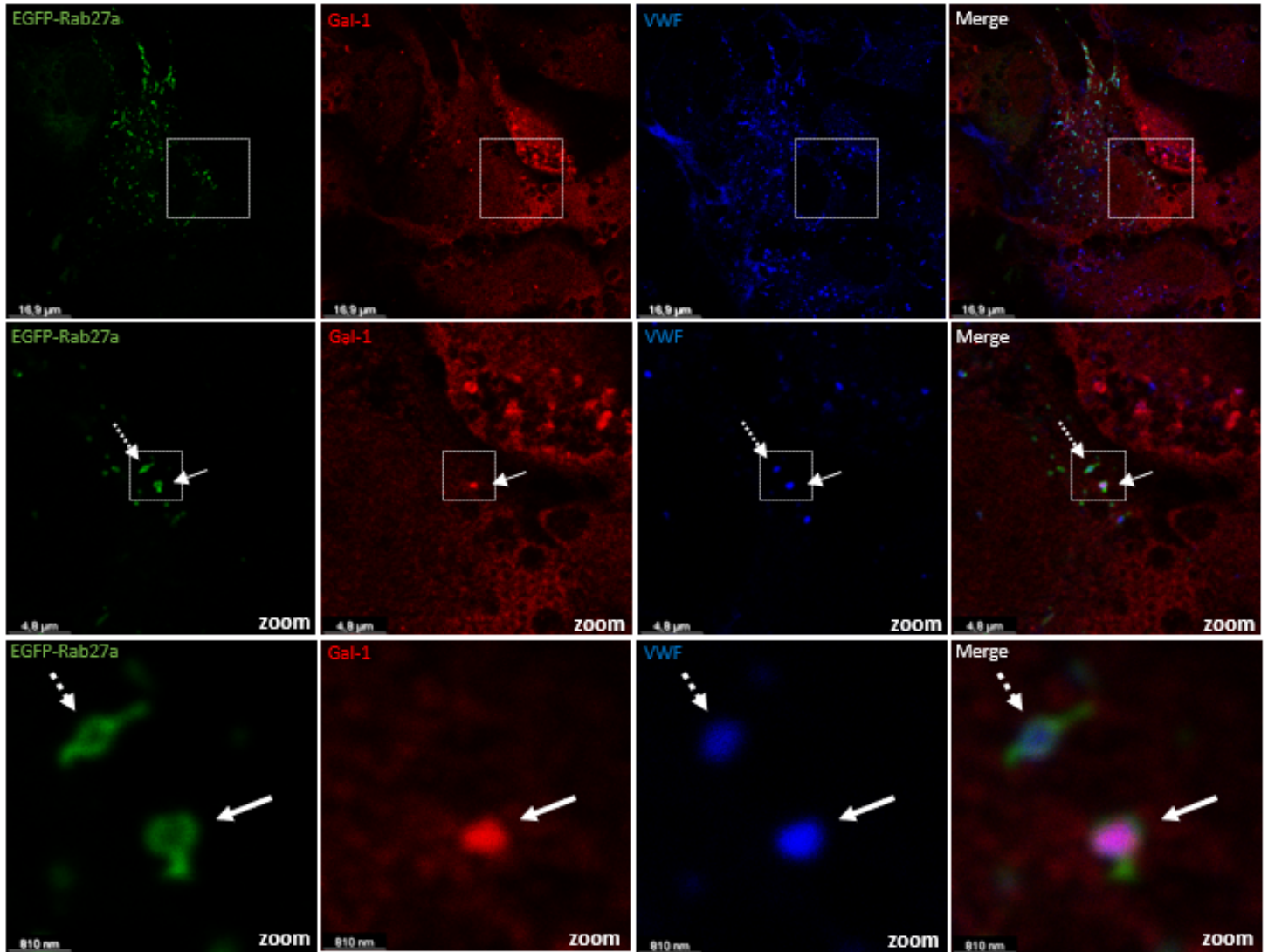
Figure 3.10- Galectin-1 is stored in the lumen of WPBs. *Triple immunofluorescence staining for EGRP-Rab27a (green), Gal-1 (red) and VWF (blue) in fixed HUVECS and observation by confocal microcopy. At zoom we observe two WPBs: with a regular arrow is a WPB where Gal-1 is present and co-localizes with VWF in the lumen, with Rab27a being in the periphery and surrounding the two proteins, and with a dashed arrow is a WPB that is not Gal-1 positive, while showing VWF in the interior and Rab27a in the periphery. The first set of images were captured with pinhole of size 1 Airy Unit (AU) whereas the last two sets of images were captured with a 0.5 AU pinhole.*

3.8 Investigation of Gal-1 entry conditions in WPBs

3.8.1 Over-confluent conditions of HUVECs induce the entry of Gal-1 into WPBs

The identification of Gal-1 in the lumen of WPBs raises interesting questions about the mechanism by which this protein, lacking an ER signal peptide (thus being unable to enter the ER-Golgi-secretory vesicle route), manages to enter and be stored in these specific secretory vesicles bypassing the classical secretory route. Given the role of galectins in recognizing membrane damage and inducing the cellular repair mechanism (Daussy & Wodrich, 2020), we hypothesized that Gal-1 positive WPBs are likely to have suffered membrane damage. This hypothesis is supported by the fact that only a subpopulation of WPBs store Gal-1, even though it is a cytoplasmic protein.

WPBs undergoing homotypic fusion may face leaky fusion, or membrane damage, as happens in other organelles, e.g. phagosomes (Yu et al., 2022), resulting in bodies with leaky (or damaged) membranes. Also, increasing confluence in *in-vitro* culture leads to an increase in the number of WPBs in cells (Howell et al., 2004), which induces homotypic fusion and thus possible leaky fusion. Therefore, we compared the number of cells positive for Gal-1 WPBs between confluent (100% confluence) and over-confluent conditions (in which we maintained cells 1, 2 or 3 days after 100% confluence), which is known to block exocytosis, thus increasing the number of WPBs per cell, which consequently increases the density of WPBs in the cytoplasm and the rate of homotypic fusion.

Figure 3.11 shows the percent of cells having positive Gal-1 WPBs in each field, for different confluence states, from three independent replicates of the assay. We observe that the number of cells positive for Gal-1 WPBs increases significantly as the number of days the cells are left in culture after reaching confluence. In contrast, between two and three days after confluent conditions, no statistically significant differences are observed, indicating that there is a plateau in the number of cells that can be positive per field. Also noteworthy is that in the confluent conditions, the percent of cells showing positive Gal-1 WPBs per field from one replicate (blue points), although consistent with each other, are much lower than cells in the other two replicates (red and green points). This heterogeneity between different cells, in untreated conditions, was frequently observed and, although the underlying cause is unclear, we hypothesize that it might be due to donor characteristics differences, eg blood group or sex, since HUVECs exhibit such characteristics (Addis et al., 2014;

Kocherova et al., 2019), or due to stress differences caused during birth and umbilical cord and cell preparation.
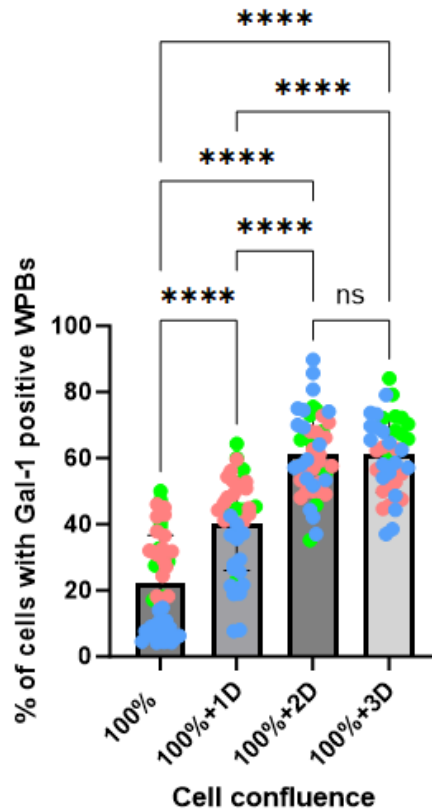
Figure 3.11- Culturing HUVECs under over-confluent conditions significantly increases the percentage of cells with Gal-1 positive WPBs. *Cells were fixed under the following conditions: 100% confluence, as well as 100% + 1 day, 100% + 2 days and 100% + 3 days post confluence, and the percentage of cells having Gal-1 positive WPBs was calculated, after immunofluorescence staining. There is a statistically significant increase in the percentage of cells with Gal-1 positive WPBs, while it seems that it reaches a plateau at 2 days post-confluence. Each point corresponds to the percentage of cells per field showing at least one Gal-1 positive WPB, and the assay was repeated three independent times, each shown in a different color (green, red and blue). In each condition (cell confluence) from each of the three assays, at least 10 fields corresponding to more than 500 cells were counted (range 472 - 957 cells per condition per assay). The statistical analysis was performed on GraphPad Prism using one-way ANOVA analysis (****-P<0.0001, ns - no significance).*

Figure 3.12 presents an example of fields showing the significant increase in Gal-1 positive WPBs, under overconfluent conditions. We observe that 3 days post full confluence, the density of WPBs rises significantly, leading to an increase in the number of WPBs storing Gal-1.
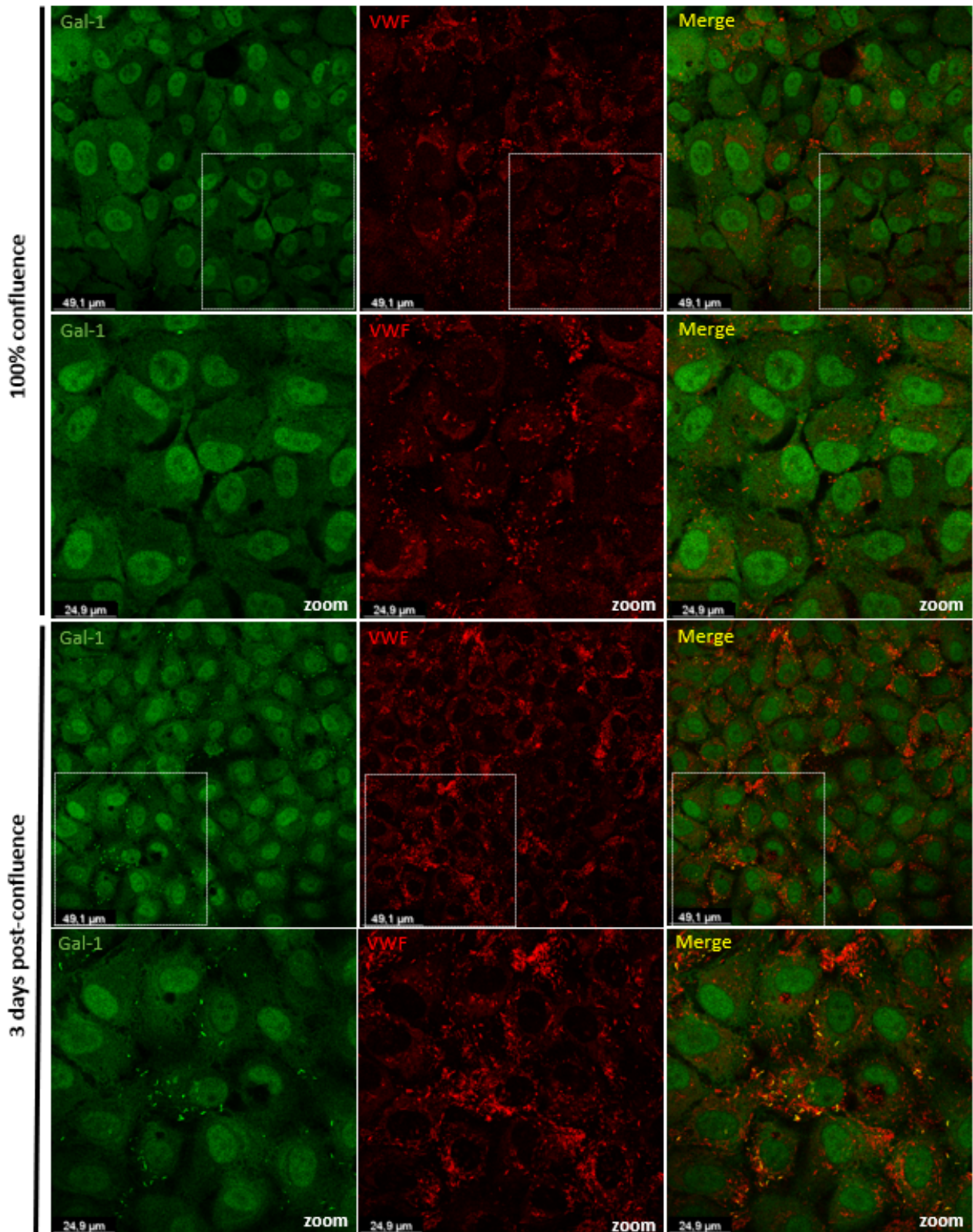
Figure 3.12- Example fields where we observe the significant increase in Gal-1 positive WPBs, 3 days after 100% confluence*. Comparison of HUVE cells fixed at 100% confluence and 3 days post full confluence, followed by immunofluorescence staining for Gal-1 (green) and VWF (red). The rise in Gal-1 positive WPBs is likely due to the significant increase in WPB density, which allows for increased leaky homotypic fusion.*

58

3.8.2 Migration of HUVECs induces the entry of Gal-1 into WPBs at the leading edge

Another way to test whether homotypic fusion, caused by increased cell density, is the cause of Gal-1 entry into WPBs, is by increasing the density of WPBs, locally in the cytoplasm, through the *in-vitro* scratch assay. In this assay, WPBs accumulate at the leading edge of cells that move to heal the artificial gap (so-called "scratch"), resulting in a significant increase in their density. This leads to an increase in homotypic fusion between WPBs and thus possibly to leaky fusion. Interestingly, we observed that in the leading edges, many Gal-1 positive WPBs were also accumulating, as shown in Figure 3.13. Particularly in Figure 3.13, where the cells were fixed 6 hrs after scratch, the first row of images shows in the left part the scratch that has not yet healed, while in the next two rows at zoom we observe that many WPBs accumulated in the leading edge, with many of them storing Gal-1 (see arrows). However, this test is an indication rather than a proof, since we did not perform a statistical analysis, as we observed a large heterogeneity in the accumulation of WPBs in the leading edge, which did not allow a statistically safe conclusion.
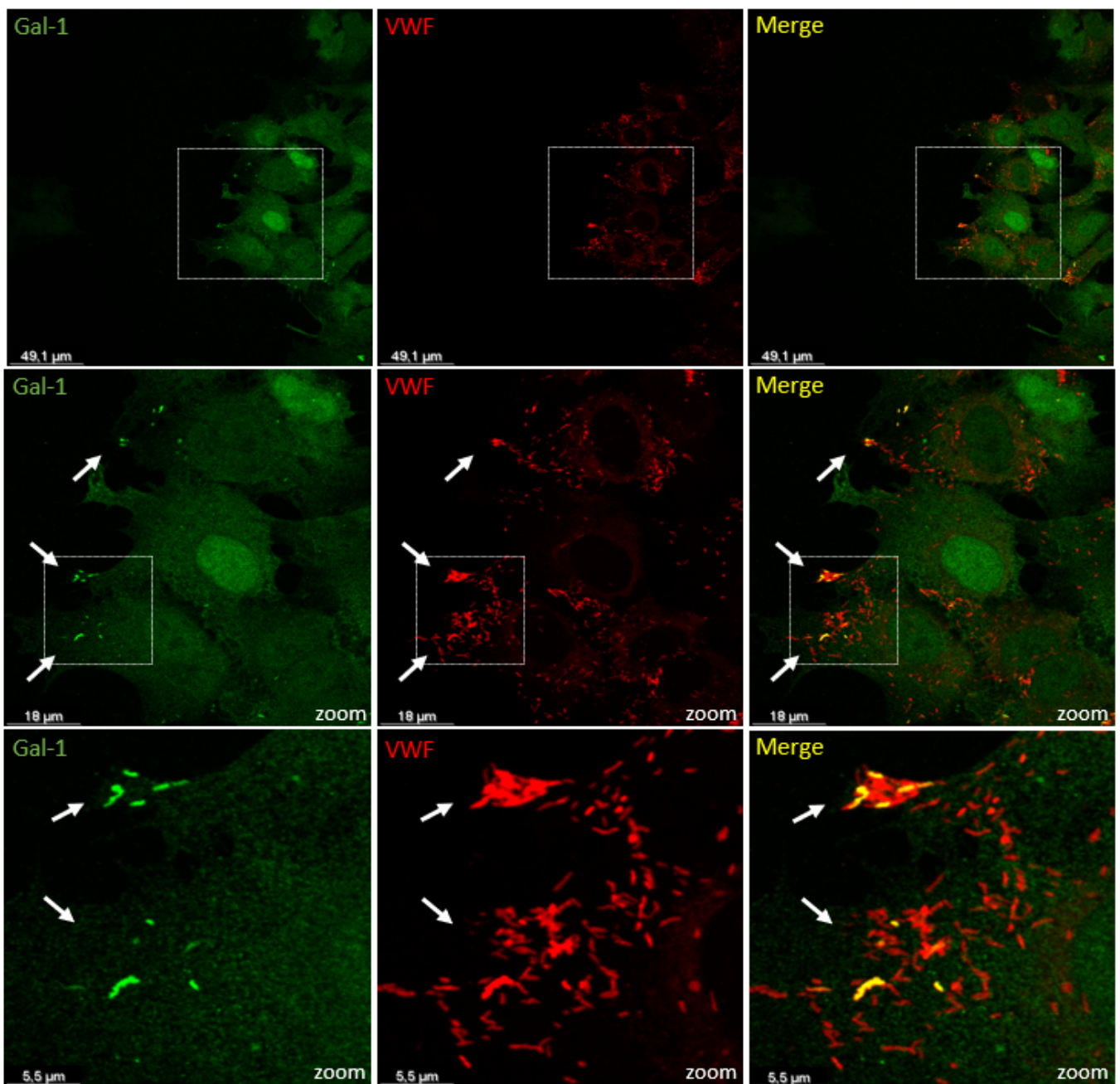
Figure 3.13 - Gal-1 is stored in WPBs at the leading edge of migrating HUVECs. *Immunofluorescence of fixed HUVECs, 6 hrs after scratch, stained for Gal-1 (green) and VWF (red) and observation by confocal microscopy. The first set of images on the left shows the scratch, with cells moving to heal it, where the characteristic elongated cell morphology can be observed. In the next two sets of zoomed images, we note that in the leading edge of the cells, where WPBs accumulate, many Gal-1 positive WPBs appear, as indicated by arrows.*

4. DISCUSSION

Previous research in our laboratory had identified the cytoplasmic protein galectin-1 (Gal-1) as a cargo of the secretory vesicles of endothelial cells, Weibel Palade bodies (WPBs). Since Gal-1 is an unconventionally secreted protein that lacks a signal peptide (a signal sequence that drives newly synthesized proteins into the Endoplasmic reticulum- Golgi secretory pathway), it was striking that Gal-1 is localized in WPBs.

In this research project, we aimed to determine the topology of Gal-1 in vesicles, i.e. whether it is located at the membrane surface facing the cytoplasmic side of WPBs, since Gal-1 is a cytoplasmic protein, or whether it is localized in their lumen, and to investigate the conditions that drive Gal-1 to WPBs.

Regarding the topology of Gal-1 in WPBs, the process was challenging enough based on the microscopy tools at our disposal. Specifically, for our study we used confocal laser scanning microscopy (CLSM) (specifically the leica sp5 microscope), which can reach 500 nm in axial resolution and 180 nm in lateral resolution under optimal conditions (Fouquet et al., 2015). This resolution is not sufficient to distinguish the lumen from the periphery of the WPB, since the vesicle has an elongated shape with a diameter of only 100-300 nm. Indeed, when a lumenal protein (e.g. VWF) is studied in combination with a membrane protein (e.g. Rab27a) by CLSM, microscopy shows complete co-localization of the two proteins (see Fig. 3.3- cartoon representation, Figure 3.4- confocal images), irrespectively of the length of the body. Thus, this technology is unable to distinguish the periphery from the lumen of the vesicle, and, consequently, to address whether Gal-1 is localized in the lumen or in the periphery of the body. Therefore, to investigate the topology of Gal-1 at WPBs we sought to convert the shape of the body from thin elongated to round, by altering the pH of the vesicles, by incubating the cells with ammonium chloride solution (NH_4Cl) for 4hrs. In particular, incubation of cells with NH_4Cl solution increases intra-WPB pH from ~5.5 to >7.4 resulting in their elongated shape being changed to rounded (Erent et al., 2007), since alkalinization of the vesicle interferes with VWF multimerization, which maintains the elongated shape of WPBs, by dissociating the dimeric bouquet of VWF (Zhou et al., 2011). The rounded WPBs have an increased diameter, thereby allowing us to resolve between the lumen and the membrane of the WPB (see Figure 3.5- cartoon representation). In fact, the longer a native WPB is, the larger diameter it will reach

upon roundness (after treatment with NH$_4$Cl), thus allowing easier discrimination between the membrane and the lumen.

Having solved the limitation issue imposed by light microscopy, we used the Rab27a protein, which is recruited outside of the WPBs during their maturation, as a membrane marker. In this way, in transfected cells (expressing EGFP-Rab27a), and triple staining, we demonstrated that Gal-1 is stored in the lumen of the vesicle along with VWF, while Rab27a appears as a "ring" around the rounded WPBs (Figures 3.9 and 3.10). This is a novel finding, and we believe it will lead to filling a gap in the literature. More specifically, although it has been reported that galectins are able to use cellular vesicles, endosomes and lysosomes, for their secretion, used as secretory vesicles for unconventional secretion (Popa et al., 2018), there is no study showing that galectins enter secretory vesicles of the conventional secretion pathway, which for vascular endothelial cells are WPBs. Also, although it has been assumed that Gal-1 may be stored in WPBs, since binding experiments using purified Gal-1 and VWF demonstrate that VWF can interact directly with Gal-1 and Duolink-PLA analysis in HUVECs showed that the two proteins colocalize within a radius of 40 nm (Saint-Lu et al., 2012), there is no direct experimental evidence showing that Gal-1 is indeed in WPBs. Here, we demonstrated not only that it is in WPBs but also that it is stored in their lumen.

Thus, an interesting question that arises is how the unconventionally secreted Gal-1 manages to directly enter, and be stored, in the lumen of secretory vesicle WPBs, which bud from the trans-Golgi network, since it does not possess a signal peptide to drive it to the ER- Golgi- WPB route. Given that it has been described in the literature that galectins are able to accumulate around damaged membrane vesicles (Hong et al., 2021) and since we observed that Gal-1 is found only in a subpopulation of WPBs, in untreaded cells, we assumed that Gal-1 positive WPBs had suffered from a damaged membrane. To test this hypothesis, we used an indirect approach; we significantly increased the density of WPBs that leads to an increase in homotypic fusion phenomena, which is likely to be leaky, as happens in other organelles, e.g. phagosomes (Yu et al., 2022). The increase in WPBs density was achieved by culturing HUVECs under overconfluent conditions (maintained up to 3 days in post-confluent culture) which inhibits the secretion of WPBs due to remodeling of actin filaments at the cell periphery. Statistical analysis of data from three independent experiments showed that

two- and three-days post-confluent, on average 60% of cells per field were positive for Gal-1 WPBs, a strikingly higher percentage in comparison to under-confluent cells or cells that just reached confluence. The density of WPBs was also increased by another assay, the scratch assay, which causes WPBs to accumulate at the leading edge of cells. Again, in areas of high WPBs density, a high percentage of these were Gal-1 positive.

These findings indicate that Gal-1 passes into WPBs from their membrane damage region and then is stored inside them, due to the ability of Gal-1 to interact with VWF sugars, as shown by binding experiments using purified Gal-1 and VWF proteins (Saint-Lu et al., 2012). However, it remains to be directly shown that membrane damage is indeed the cause of Gal-1 entry into WPBs, by directly inducing vesicle membrane destruction e.g. by introducing crystals into WPBs, or protein aggregates or bacterial pore forming toxins.

In conclusion, we believe that this study, which demonstrates that galectin-1 is able to be stored in the lumen of WPBs, initiates a new avenue in understanding unconventional secretion of proteins, in particular the family of galectins, which play a key role in a variety of functions inside and outside cells (Popa et al., 2018) . Our demonstration that Gal-1 enters WPBs that have suffered membrane damage is consistent with the view that the secretion of galectins results from stress conditions for the cell (Popa et al., 2018), since they can use damaged vesicles as means of exocytosis. We pioneeringly add another type of vesicles that can be used for exocytosis, WPBs, which strikingly are vesicles used for the conventional protein secretion pathway.

REFERENCES

Addis, R., Campesi, I., Fois, M., Capobianco, G., Dessole, S., Fenu, G., Montella, A., Cattaneo, M. G., Vicentini, L. M., & Franconi, F. (2014). Human umbilical endothelial cells (HUVECs) have a sex: Characterisation of the phenotype of male and female cells. *Biology of Sex Differences*, *5*(1), 18. https://doi.org/10.1186/s13293-014-0018-2

Andrejecsk, J. W., Cui, J., Chang, W. G., Devalliere, J., Pober, J. S., & Saltzman, W. M. (2013). Paracrine exchanges of molecular signals between alginate-encapsulated pericytes and freely suspended endothelial cells within a 3D protein gel. *Biomaterials*, *34*(35), 8899–8908. https://doi.org/10.1016/j.biomaterials.2013.08.008

Babich, V., Meli, A., Knipe, L., Dempster, J. E., Skehel, P., Hannah, M. J., & Carter, T. (2008). Selective release of molecules from Weibel-Palade bodies during a lingering kiss. *Blood*, *111*(11), 5282–5290. https://doi.org/10.1182/blood-2007-09-113746

Barondes, S. H., Castronovo, V., Cooper, D. N. W., Cummings, R. D., Drickamer, K., Felzi, T., Gitt, M. A., Hirabayashi, J., Hughes, C., Kasai, K., Leffler, H., Liu, F.-T., Lotan, R., Mercurio, A. M., Monsigny, M., Pillai, S., Poirer, F., Raz, A., Rigby, P. W. J., … Wang, J. L. (1994). Galectins: A family of animal β-galactoside-binding lectins. *Cell*, *76*(4), 597–598. https://doi.org/10.1016/0092-8674(94)90498-7

Baudin, B., Bruneel, A., Bosselut, N., & Vaubourdolle, M. (2007). A protocol for isolation and culture of human umbilical vein endothelial cells. *Nature Protocols*, *2*(3), 481–485. https://doi.org/10.1038/nprot.2007.54

Bierings, R., Hellen, N., Kiskin, N., Knipe, L., Fonseca, A.-V., Patel, B., Meli, A., Rose, M., Hannah, M. J., & Carter, T. (2012). The interplay between the Rab27A effectors Slp4-a and MyRIP controls hormone-evoked Weibel-Palade body exocytosis. *Blood*, *120*(13), 2757–2767. https://doi.org/10.1182/blood-2012-05-429936

Boerma, M., Burton, G. R., Wang, J., Fink, L. M., McGehee, R. E., & Hauer-Jensen, M. (2006). Comparative expression profiling in primary and immortalized endothelial cells: Changes in gene expression in response to hydroxy methylglutaryl-coenzyme A reductase inhibition. *Blood Coagulation & Fibrinolysis*, *17*(3), 173–180. https://doi.org/10.1097/01.mbc.0000220237.99843.a1

Bowman, S. L., Bi-Karchin, J., Le, L., & Marks, M. S. (2019). The road to lysosome-related organelles: Insights from Hermansky-Pudlak syndrome and other rare diseases. *Traffic*, *20*(6), 404–435. https://doi.org/10.1111/tra.12646

Camby, I., Le Mercier, M., Lefranc, F., & Kiss, R. (2006). Galectin-1: A small protein with major functions. *Glycobiology*, *16*(11), 137R-157R. https://doi.org/10.1093/glycob/cwl025

Canis, K., McKinnon, T. A. J., Nowak, A., Haslam, S. M., Panico, M., Morris, H. R., Laffan, M. A., & Dell, A. (2012). Mapping the N-glycome of human von Willebrand factor. *Biochemical Journal*, *447*(2), 217–228. https://doi.org/10.1042/BJ20120810

Caniuguir, A., Krause, B. J., Hernandez, C., Uauy, R., & Casanello, P. (2016). Markers of early endothelial dysfunction in intrauterine growth restriction-derived human umbilical vein endothelial cells revealed by 2D-DIGE and mass spectrometry analyses. *Placenta*, *41*, 14–26. https://doi.org/10.1016/j.placenta.2016.02.016

Chehab, T., Santos, N. C., Holthenrich, A., Koerdt, S. N., Disse, J., Schuberth, C., Nazmi, A. R., Neeft, M., Koch, H., Man, K. N. M., Wojcik, S. M., Martin, T. F. J., Van Der Sluijs, P., Brose, N., & Gerke, V. (2017). A novel Munc13-4/S100A10/annexin A2 complex promotes Weibel–Palade body exocytosis in endothelial cells. *Molecular Biology of the Cell*, *28*(12), 1688–1700. https://doi.org/10.1091/mbc.e17-02-0128

Chowdhury, F., Howat, W. J., Phillips, G. J., & Lackie, P. M. (2010). Interactions between endothelial cells and epithelial cells in a combined cell model of airway mucosa: Effects on tight junction permeability. *Experimental Lung Research*, *36*(1), 1–11. https://doi.org/10.3109/01902140903026582

Cleator, J. H., Zhu, W. Q., Vaughan, D. E., & Hamm, H. E. (2006). Differential regulation of

endothelial exocytosis of P-selectin and von Willebrand factor by protease-activated

receptors and cAMP. *Blood*, *107*(7), 2736–2744. https://doi.org/10.1182/blood-

2004-07-2698

Conte, I. L., Hellen, N., Bierings, R., Mashanov, G. I., Manneville, J.-B., Kiskin, N. I., Hannah, M.

J., Molloy, J. E., & Carter, T. (2015). Interaction between MyRIP and the actin

cytoskeleton regulates Weibel-Palade body trafficking and exocytosis. *Journal of Cell

Science*, jcs.178285. https://doi.org/10.1242/jcs.178285

Cousin, J., & Cloninger, M. (2016). The Role of Galectin-1 in Cancer Progression, and

Synthetic Multivalent Systems for the Study of Galectin-1. *International Journal of

Molecular Sciences*, *17*(9), 1566. https://doi.org/10.3390/ijms17091566

Daussy, C. F., & Wodrich, H. (2020). "Repair Me if You Can": Membrane Damage, Response,

and Control from the Viral Perspective. *Cells*, *9*(9), 2042.

https://doi.org/10.3390/cells9092042

Delacour, D., Koch, A., & Jacob, R. (2009). The Role of Galectins in Protein Trafficking. *Traffic*,

10(10), 1405–1413. https://doi.org/10.1111/j.1600-0854.2009.00960.x

Denis, C. V., André, P., Saffaripour, S., & Wagner, D. D. (2001). Defect in regulated secretion of

P-selectin affects leukocyte recruitment in von Willebrand factor-deficient mice.

Proceedings of the National Academy of Sciences, *98*(7), 4072–4077.

https://doi.org/10.1073/pnas.061307098

Elola, M. T., Wolfenstein-Todel, C., Troncoso, M. F., Vasta, G. R., & Rabinovich, G. A. (2007).

Galectins: Matricellular glycan-binding proteins linking cell adhesion, migration, and

survival. *Cellular and Molecular Life Sciences*, *64*(13), 1679–1700.

https://doi.org/10.1007/s00018-007-7044-8

Erent, M., Meli, A., Moisoi, N., Babich, V., Hannah, M. J., Skehel, P., Knipe, L., Zupancic, G.,

Ogden, D., & Carter, T. (2007). Rate, extent and concentration dependence of

histamine-evoked Weibel-Palade body exocytosis determined from individual fusion

events in human endothelial cells. *The Journal of Physiology*, *583*(Pt 1), 195–212.

https://doi.org/10.1113/jphysiol.2007.132993

Ewenstein, B. M., Warhol, M. J., Handin, R. I., & Pober, J. S. (1987). Composition of the von

Willebrand factor storage organelle (Weibel-Palade body) isolated from cultured

human umbilical vein endothelial cells. *The Journal of Cell Biology*, *104*(5), 1423–

1433. https://doi.org/10.1083/jcb.104.5.1423

Fajka-Boja, R., Urbán, V. S., Szebeni, G. J., Czibula, Á., Blaskó, A., Kriston-Pál, É., Makra, I.,

Hornung, Á., Szabó, E., Uher, F., Than, N. G., & Monostori, É. (2016). Galectin-1 is a

local but not systemic immunomodulatory factor in mesenchymal stromal cells.

Cytotherapy, *18*(3), 360–370. https://doi.org/10.1016/j.jcyt.2015.12.004

Félétou, M., & Vanhoutte, P. M. (2006). Endothelial dysfunction: A multifaceted disorder (The

Wiggers Award Lecture). *American Journal of Physiology-Heart and Circulatory

Physiology*, *291*(3), H985–H1002. https://doi.org/10.1152/ajpheart.00292.2006

Florey. (1966). The endothelial cell. *BMJ*, *2*(5512), 487–490.

https://doi.org/10.1136/bmj.2.5512.487

Fouquet, C., Gilles, J.-F., Heck, N., Dos Santos, M., Schwartzmann, R., Cannaya, V., Morel, M.-

P., Davidson, R. S., Trembleau, A., & Bolte, S. (2015). Improving Axial Resolution in

Confocal Microscopy with New High Refractive Index Mounting Media. *PLOS ONE*,

10(3), e0121096. https://doi.org/10.1371/journal.pone.0121096

Giblin, J. P., Hewlett, L. J., & Hannah, M. J. (2008). Basal secretion of von Willebrand factor

from human endothelial cells. *Blood*, *112*(4), 957–964.

https://doi.org/10.1182/blood-2007-12-130740

Goligorsky, M. S. (2005). Endothelial cell dysfunction: Can't live with it, how to live without it.

American Journal of Physiology-Renal Physiology, *288*(5), F871–F880.

https://doi.org/10.1152/ajprenal.00333.2004

Heiss, M., Hellström, M., Kalén, M., May, T., Weber, H., Hecker, M., Augustin, H. G., & Korff, T. (2015). Endothelial cell spheroids as a versatile tool to study angiogenesis *in vitro*. *The FASEB Journal*, *29*(7), 3076–3084. https://doi.org/10.1096/fj.14-267633

Henderson, N. C., & Sethi, T. (2009). The regulation of inflammation by galectin-3. *Immunological Reviews*, *230*(1), 160–171. https://doi.org/10.1111/j.1600-065X.2009.00794.x

Hong, M.-H., Weng, I.-C., Li, F.-Y., Lin, W.-H., & Liu, F.-T. (2021). Intracellular galectins sense cytosolically exposed glycans as danger and mediate cellular responses. *Journal of Biomedical Science*, *28*(1), 16. https://doi.org/10.1186/s12929-021-00713-x

Howell, G. J., Herbert, S. P., Smith, J. M., Mittar, S., Ewan, L. C., Mohammed, M., Hunter, A. R., Simpson, N., Turner, A. J., Zachary, I., Walker, J. H., & Ponnambalam, S. (2004). Endothelial cell confluence regulates Weibel-Palade body formation. *Molecular Membrane Biology*, *21*(6), 413–421. https://doi.org/10.1080/09687860400011571

Huang, R.-H., Wang, Y., Roth, R., Yu, X., Purvis, A. R., Heuser, J. E., Egelman, E. H., & Sadler, J. E. (2008). Assembly of Weibel–Palade body-like tubules from N-terminal domains of von Willebrand factor. *Proceedings of the National Academy of Sciences*, *105*(2), 482–487. https://doi.org/10.1073/pnas.0710079105

Jang, J., Jung, Y., Kim, Y., Jho, E.-H., & Yoon, Y. (2017). LPS-induced inflammatory response is suppressed by Wnt inhibitors, Dickkopf-1 and LGK974. *Scientific Reports*, *7*, 41612. https://doi.org/10.1038/srep41612

Katsumi, A., Tuley, E. A., Bodó, I., & Sadler, J. E. (2000). Localization of Disulfide Bonds in the Cystine Knot Domain of Human von Willebrand Factor. *Journal of Biological Chemistry*, *275*(33), 25585–25594. https://doi.org/10.1074/jbc.M002654200

Kiskin, N. I., Babich, V., Knipe, L., Hannah, M. J., & Carter, T. (2014). Differential Cargo Mobilisation within Weibel-Palade Bodies after Transient Fusion with the Plasma

Membrane. *PLoS ONE*, *9*(9), e108093.

https://doi.org/10.1371/journal.pone.0108093

Kiskin, N. I., Hellen, N., Babich, V., Hewlett, L., Knipe, L., Hannah, M. J., & Carter, T. (2010).

Protein mobilities and P-selectin storage in Weibel–Palade bodies. *Journal of Cell*

Science, *123*(17), 2964–2975. https://doi.org/10.1242/jcs.073593

Knipe, L., Meli, A., Hewlett, L., Bierings, R., Dempster, J., Skehel, P., Hannah, M. J., & Carter, T.

(2010). A revised model for the secretion of tPA and cytokines from cultured

endothelial cells. *Blood*, *116*(12), 2183–2191. https://doi.org/10.1182/blood-2010-

03-276170

Kobayashi, T., Vischer, U. M., Rosnoblet, C., Lebrand, C., Lindsay, M., Parton, R. G., Kruithof, E.

K. O., & Gruenberg, J. (2000). The Tetraspanin CD63/lamp3 Cycles between

Endocytic and Secretory Compartments in Human Endothelial Cells. *Molecular*

Biology of the Cell, *11*(5), 1829–1843. https://doi.org/10.1091/mbc.11.5.1829

Kocherova, I., Bryja, A., Mozdziak, P., Angelova Volponi, A., Dyszkiewicz-Konwińska, M.,

Piotrowska-Kempisty, H., Antosik, P., Bukowska, D., Bruska, M., Iżycki, D., Zabel, M.,

Nowicki, M., & Kempisty, B. (2019). Human Umbilical Vein Endothelial Cells (HUVECs)

Co-Culture with Osteogenic Cells: From Molecular Communication to Engineering

Prevascularised Bone Grafts. *Journal of Clinical Medicine*, *8*(10), 1602.

https://doi.org/10.3390/jcm8101602

Lenting, P. J., Christophe, O. D., & Denis, C. V. (2015). von Willebrand factor biosynthesis,

secretion, and clearance: Connecting the far ends. *Blood*, *125*(13), 2019–2028.

https://doi.org/10.1182/blood-2014-06-528406

Li, P., Wei, G., Cao, Y., Deng, Q., Han, X., Huang, X., Huo, Y., He, Y., Chen, L., & Luo, J. (2018).

Myosin IIa is critical for cAMP-mediated endothelial secretion of von Willebrand

factor. *Blood*, *131*(6), 686–698. https://doi.org/10.1182/blood-2017-08-802140

Lopes Da Silva, M., & Cutler, D. F. (2016). Von Willebrand factor multimerization and the

polarity of secretory pathways in endothelial cells. *Blood*, *128*(2), 277–285.

https://doi.org/10.1182/blood-2015-10-677054

Lowenstein, C. J., Morrell, C. N., & Yamakuchi, M. (2005). Regulation of Weibel–Palade Body

Exocytosis. *Trends in Cardiovascular Medicine*, *15*(8), 302–308.

https://doi.org/10.1016/j.tcm.2005.09.005

Luft, J. H. (1966). Fine structures of capillary and endocapillary layer as revealed by

ruthenium red. *Federation Proceedings*, *25*(6), 1773–1783.

Ma, J., Zhang, Z., Yang, L., Kriston-Vizi, J., Cutler, D. F., & Li, W. (2016). BLOC-2 subunit HPS6

deficiency affects the tubulation and secretion of von Willebrand factor from mouse

endothelial cells. *Journal of Genetics and Genomics*, *43*(12), 686–693.

https://doi.org/10.1016/j.jgg.2016.09.007

Manjithaya, R., & Subramani, S. (2011). Autophagy: A broad role in unconventional protein

secretion? *Trends in Cell Biology*, *21*(2), 67–73.

https://doi.org/10.1016/j.tcb.2010.09.009

Marin, V., Kaplanski, G., Grès, S., Farnarier, C., & Bongrand, P. (2001). Endothelial cell culture:

Protocol to obtain and cultivate human umbilical endothelial cells. *Journal of

Immunological Methods*, *254*(1–2), 183–190. https://doi.org/10.1016/S0022-

1759(01)00408-2

McCormack, J. J., Lopes Da Silva, M., Ferraro, F., Patella, F., & Cutler, D. F. (2017).

Weibel–Palade bodies at a glance. *Journal of Cell Science*, *130*(21), 3611–3617.

https://doi.org/10.1242/jcs.208033

Michaux, G., & Cutler, D. F. (2004). How to Roll an Endothelial Cigar: The Biogenesis of

Weibel-Palade Bodies. *Traffic*, *5*(2), 69–78. https://doi.org/10.1111/j.1600-

0854.2004.00157.x

Mourik, M. J., Faas, F. G. A., Zimmermann, H., Voorberg, J., Koster, A. J., & Eikenboom, J.

   (2015). Content delivery to newly forming Weibel-Palade bodies is facilitated by

   multiple connections with the Golgi apparatus. *Blood*, *125*(22), 3509–3516.

   https://doi.org/10.1182/blood-2014-10-608596

Mourik, M. J., Valentijn, J. A., Voorberg, J., Koster, A. J., Valentijn, K. M., & Eikenboom, J.

   (2013). Von Willebrand factor remodeling during exocytosis from vascular

   endothelial cells. *Journal of Thrombosis and Haemostasis*, *11*(11), 2009–2019.

   https://doi.org/10.1111/jth.12401

Naß, J., Terglane, J., & Gerke, V. (2021). Weibel Palade Bodies: Unique Secretory Organelles

   of Endothelial Cells that Control Blood Vessel Homeostasis. *Frontiers in Cell and

   Developmental Biology*, *9*, 813995. https://doi.org/10.3389/fcell.2021.813995

Nickel, W., & Rabouille, C. (2009). Mechanisms of regulated unconventional protein

   secretion. *Nature Reviews Molecular Cell Biology*, *10*(2), 148–155.

   https://doi.org/10.1038/nrm2617

Nightingale, T. D., Pattni, K., Hume, A. N., Seabra, M. C., & Cutler, D. F. (2009). Rab27a and

   MyRIP regulate the amount and multimeric state of VWF released from endothelial

   cells. *Blood*, *113*(20), 5010–5018. https://doi.org/10.1182/blood-2008-09-181206

Nightingale, T. D., White, I. J., Doyle, E. L., Turmaine, M., Harrison-Lavoie, K. J., Webb, K. F.,

   Cramer, L. P., & Cutler, D. F. (2011). Actomyosin II contractility expels von Willebrand

   factor from Weibel–Palade bodies during exocytosis. *Journal of Cell Biology*, *194*(4),

   613–629. https://doi.org/10.1083/jcb.201011119

Palade, G. (1975). Intracellular Aspects of the Process of Protein Synthesis. *Science*,

   189(4200), 347–358. https://doi.org/10.1126/science.1096303

Pannekoek, H., & Voorberg, J. (1989). 5 Molecular cloning, expression and assembly of

   multimeric von Willebrand factor. *Baillière's Clinical Haematology*, *2*(4), 879–896.

   https://doi.org/10.1016/S0950-3536(89)80050-2

Paroutis, P., Touret, N., & Grinstein, S. (2004). The pH of the Secretory Pathway: Measurement, Determinants, and Regulation. *Physiology*, *19*(4), 207–215. https://doi.org/10.1152/physiol.00005.2004

Patel, H., Chen, J., Das, K. C., & Kavdia, M. (2013). Hyperglycemia induces differential change in oxidative stress at gene expression and functional levels in HUVEC and HMVEC. *Cardiovascular Diabetology*, *12*(1), 142. https://doi.org/10.1186/1475-2840-12-142

Popa, S. J., Stewart, S. E., & Moreau, K. (2018). Unconventional secretion of annexins and galectins. *Seminars in Cell & Developmental Biology*, *83*, 42–50. https://doi.org/10.1016/j.semcdb.2018.02.022

Pries, A. R., Secomb, T. W., & Gaehtgens, P. (2000). The endothelial surface layer. *Pflügers Archiv - European Journal of Physiology*, *440*(5), 653–666. https://doi.org/10.1007/s004240000307

Rabouille, C. (2017). Pathways of Unconventional Protein Secretion. *Trends in Cell Biology*, *27*(3), 230–240. https://doi.org/10.1016/j.tcb.2016.11.007

Rabouille, C., Malhotra, V., & Nickel, W. (2012). Diversity in unconventional protein secretion. *Journal of Cell Science*, *125*(22), 5251–5255. https://doi.org/10.1242/jcs.103630

Saint-Lu, N., Oortwijn, B. D., Pegon, J. N., Odouard, S., Christophe, O. D., De Groot, P. G., Denis, C. V., & Lenting, P. J. (2012). Identification of Galectin-1 and Galectin-3 as Novel Partners for Von Willebrand Factor. *Arteriosclerosis, Thrombosis, and Vascular Biology*, *32*(4), 894–901. https://doi.org/10.1161/ATVBAHA.111.240309

Samor, B., Michalski, J.-C., Mazurier, C., Goudemand, M., De Waard, P., Vliegenthart, J. F. G., Strecker, G., & Montreuil, J. (1989). Primary structure of the majorO-glycosidically linked carbohydrate unit of human von Willebrand factor. *Glycoconjugate Journal*, *6*(3), 263–270. https://doi.org/10.1007/BF01047846

Schillemans, M., Karampini, E., Kat, M., & Bierings, R. (2019). Exocytosis of Weibel–Palade

bodies: How to unpack a vascular emergency kit. *Journal of Thrombosis and*

Haemostasis, *17*(1), 6–18. https://doi.org/10.1111/jth.14322

Shapiro, S. E., Nowak, A. A., Wooding, C., Birdsey, G., Laffan, M. A., & McKinnon, T. A. J.

(2014). The von Willebrand factor predicted unpaired cysteines are essential for

secretion. *Journal of Thrombosis and Haemostasis*, *12*(2), 246–254.

https://doi.org/10.1111/jth.12466

Sharda, A. V., Barr, A. M., Harrison, J. A., Wilkie, A. R., Fang, C., Mendez, L. M., Ghiran, I. C.,

Italiano, J. E., & Flaumenhaft, R. (2020). VWF maturation and release are controlled

by 2 regulators of Weibel-Palade body biogenesis: Exocyst and BLOC-2. *Blood*,

136(24), 2824–2837. https://doi.org/10.1182/blood.2020005300

Sporn, L. A., Marder, V. J., & Wagner, D. D. (1986). Inducible secretion of large, biologically

potent von Willebrand factor multimers. *Cell*, *46*(2), 185–190.

https://doi.org/10.1016/0092-8674(86)90735-X

Stillman, B. N., Hsu, D. K., Pang, M., Brewer, C. F., Johnson, P., Liu, F.-T., & Baum, L. G. (2006).

Galectin-3 and Galectin-1 Bind Distinct Cell Surface Glycoprotein Receptors to Induce

T Cell Death. *The Journal of Immunology*, *176*(2), 778–789.

https://doi.org/10.4049/jimmunol.176.2.778

Sundblad, V., Morosi, L. G., Geffner, J. R., & Rabinovich, G. A. (2017). Galectin-1: A Jack-of-All-

Trades in the Resolution of Acute and Chronic Inflammation. *The Journal of*

Immunology, *199*(11), 3721–3730. https://doi.org/10.4049/jimmunol.1701172

Valentijn, K. M., & Eikenboom, J. (2013). Weibel–Palade bodies: A window to von Willebrand

disease. *Journal of Thrombosis and Haemostasis*, *11*(4), 581–592.

https://doi.org/10.1111/jth.12160

Valentijn, K. M., Valentijn, J. A., Jansen, K. A., & Koster, A. J. (2008). A new look at Weibel–

Palade body structure in endothelial cells using electron tomography. *Journal of*

Structural Biology, *161*(3), 447–458. https://doi.org/10.1016/j.jsb.2007.08.001

Valentijn, K. M., Van Driel, L. F., Mourik, M. J., Hendriks, G.-J., Arends, T. J., Koster, A. J., &

Valentijn, J. A. (2010). Multigranular exocytosis of Weibel-Palade bodies in vascular

endothelial cells. *Blood*, *116*(10), 1807–1816. https://doi.org/10.1182/blood-2010-

03-274209

Van Agtmaal, E. L., Bierings, R., Dragt, B. S., Leyen, T. A., Fernandez-Borja, M., Horrevoets, A.

J. G., & Voorberg, J. (2012). The Shear Stress-Induced Transcription Factor KLF2

Affects Dynamics and Angiopoietin-2 Content of Weibel-Palade Bodies. *PLoS ONE*,

7(6), e38399. https://doi.org/10.1371/journal.pone.0038399

Van Breevoort, D., Snijders, A. P., Hellen, N., Weckhuysen, S., Van Hooren, K. W. E. M.,

Eikenboom, J., Valentijn, K., Fernandez-Borja, M., Ceulemans, B., De Jonghe, P.,

Voorberg, J., Hannah, M., Carter, T., & Bierings, R. (2014). STXBP1 promotes Weibel-

Palade body exocytosis through its interaction with the Rab27A effector Slp4-a.

Blood, *123*(20), 3185–3194. https://doi.org/10.1182/blood-2013-10-535831

Van Der Wouden, J. M., Maier, O., Van IJzendoorn, S. C. D., & Hoekstra, D. (2003). Membrane

Dynamics and the Regulation of Epithelial Cell Polarity. In *International Review of*

Cytology (Vol. 226, pp. 127–164). Elsevier. https://doi.org/10.1016/S0074-

7696(03)01003-9

Vasta, G. R. (2012). Galectins as Pattern Recognition Receptors: Structure, Function, and

Evolution. In J. D. Lambris & G. Hajishengallis (Eds.), *Current Topics in Innate*

Immunity II (Vol. 946, pp. 21–36). Springer New York. https://doi.org/10.1007/978-1-

4614-0106-3_2

Verweij, C. L., Hart, M., & Pannekoek, H. (1987). Expression of variant von Willebrand factor

(vWF) cDNA in heterologous cells: Requirement of the pro-polypeptide in vWF

multimer formation. *The EMBO Journal*, *6*(10), 2885–2890.

https://doi.org/10.1002/j.1460-2075.1987.tb02591.x

Viguier, M., Advedissian, T., Delacour, D., Poirier, F., & Deshayes, F. (2014). Galectins in

epithelial functions. *Tissue Barriers*, *2*(3), e29103.

https://doi.org/10.4161/tisb.29103

Villalba, N., Baby, S., & Yuan, S. Y. (2021). The Endothelial Glycocalyx as a Double-Edged

Sword in Microvascular Homeostasis and Pathogenesis. *Frontiers in Cell and*

Developmental Biology, *9*, 711003. https://doi.org/10.3389/fcell.2021.711003

Vischer, U. M., Barth, H., & Wollheim, C. B. (2000). Regulated von Willebrand Factor

Secretion Is Associated With Agonist-Specific Patterns of Cytoskeletal Remodeling in

Cultured Endothelial Cells. *Arteriosclerosis, Thrombosis, and Vascular Biology*, *20*(3),

883–891. https://doi.org/10.1161/01.ATV.20.3.883

Voorberg, J., Fontijn, R., Calafat, J., Janssen, H., Van Mourik, J. A., & Pannekoek, H. (1993).

Biogenesis of von Willebrand factor-containing organelles in heterologous

transfected CV-1 cells. *The EMBO Journal*, *12*(2), 749–758.

https://doi.org/10.1002/j.1460-2075.1993.tb05709.x

Wagner, D. D., Saffaripour, S., Bonfanti, R., Sadler, J. E., Cramer, E. M., Chapman, B., &

Mayadas, T. N. (1991). Induction of specific storage organelles by von Willebrand

factor propolypeptide. *Cell*, *64*(2), 403–413. https://doi.org/10.1016/0092-

8674(91)90648-I

Walshe, T. E., Dela Paz, N. G., & D'Amore, P. A. (2013). The Role of Shear-Induced

Transforming Growth Factor-β Signaling in the Endothelium. *Arteriosclerosis,*

Thrombosis, and Vascular Biology, *33*(11), 2608–2617.

https://doi.org/10.1161/ATVBAHA.113.302161

Weibel, E. R. (2012). Fifty years of Weibel–Palade bodies: The discovery and early history of

an enigmatic organelle of endothelial cells. *Journal of Thrombosis and Haemostasis*,

10(6), 979–984. https://doi.org/10.1111/j.1538-7836.2012.04718.x

Weibel, E. R., & Palade, G. E. (1964). NEW CYTOPLASMIC COMPONENTS IN ARTERIAL

ENDOTHELIA. *The Journal of Cell Biology*, *23*(1), 101–112.

https://doi.org/10.1083/jcb.23.1.101

Wise, R. J., Barr, P. J., Wong, P. A., Kiefer, M. C., Brake, A. J., & Kaufman, R. J. (1990).

Expression of a human proprotein processing enzyme: Correct cleavage of the von

Willebrand factor precursor at a paired basic amino acid site. *Proceedings of the*

National Academy of Sciences, *87*(23), 9378–9382.

https://doi.org/10.1073/pnas.87.23.9378

Yang, R.-Y., Rabinovich, G. A., & Liu, F.-T. (2008). Galectins: Structure, function and

therapeutic potential. *Expert Reviews in Molecular Medicine*, *10*, e17.

https://doi.org/10.1017/S1462399408000719

Yano, K., Gale, D., Massberg, S., Cheruvu, P. K., Monahan-Earley, R., Morgan, E. S., Haig, D.,

Von Andrian, U. H., Dvorak, A. M., & Aird, W. C. (2007). Phenotypic heterogeneity is

an evolutionarily conserved feature of the endothelium. *Blood*, *109*(2), 613–615.

https://doi.org/10.1182/blood-2006-05-026401

Yu, Y., Jiao, M., Zhang, Z., & Yu, Y. (2022). Single-phagosome imaging reveals that homotypic

fusion impairs phagosome degradative function. *Biophysical Journal*, *121*(3), 459–

469. https://doi.org/10.1016/j.bpj.2021.12.032

Zenner, H. L., Collinson, L. M., Michaux, G., & Cutler, D. F. (2007). High-pressure freezing

provides insights into Weibel-Palade body biogenesis. *Journal of Cell Science*,

120(12), 2117–2125. https://doi.org/10.1242/jcs.007781

Zhou, Y.-F., Eng, E. T., Nishida, N., Lu, C., Walz, T., & Springer, T. A. (2011). A pH-regulated

dimeric bouquet in the structure of von Willebrand factor: A pH-regulated dimeric

bouquet in VWF. *The EMBO Journal*, *30*(19), 4098–4111.

https://doi.org/10.1038/emboj.2011.297

Zhou, Y.-F., Eng, E. T., Zhu, J., Lu, C., Walz, T., & Springer, T. A. (2012). Sequence and structure

relationships within von Willebrand factor. *Blood*, *120*(2), 449–458.

https://doi.org/10.1182/blood-2012-01-405134

Zografou, S., Basagiannis, D., Papafotika, A., Shirakawa, R., Horiuchi, H., Auerbach, D.,

Fukuda, M., & Christoforidis, S. (2012). Rab-genome analysis reveals novel insights in

Weibel-Palade body exocytosis. *Journal of Cell Science*, jcs.104174.

https://doi.org/10.1242/jcs.104174